Nanostructured Porous Silicon Scaffolds for Enhanced Biocompatibility of Multichannel Microelectrodes

A Thesis

Submitted to the Faculty

of

Drexel University

by

Stefanie Joy Hallman

in partial fulfillment of the

requirements for the degree

of

Master of Science in Biomedical Engineering

May 2009

Acknowledgements

Foremost, I would like to thank my advisor, Dr. Karen Moxon, for her assistance and oversight of all my research endeavors for the last four years. Her thoughtful feedback on my work during this time has allowed me to develop the inquiring mindset and scientific thought processes imperative for an engineer and a researcher.

Additionally, I would like to thank my committee members, Drs. Kenneth Barbee and Bahrad Sokhansanj for their guidance in completing and clarifying this document.

Many people have contributed to the methods developed and results obtained for this document. I would like to thank Drs. Timothy Himes and Chuma Okere from the Department of Neurobiology and Anatomy at the Drexel University College of Medicine for their assistance in learning the techniques required for the successful completion of histology, immunohistochemistry, and fluorescence microscopy. Also, I would like to thank Eric Knudsen for utilizing his MATLAB expertise to bring our quantification protocol into reality.

TABLE OF CONTENTS

LIST OF TABLES

LIST OF FIGURES

ABSTRACT

Nanostructured Porous Silicon Scaffolds for
Enhanced Biocompatibility of Multichannel Microelectrodes

Stefanie Joy Hallman
Karen Moxon, Ph.D.

Many different types of microelectrodes have been developed for use as a direct Brain-Machine Interface (BMI) to chronically record single- neuron action potentials from ensembles of neurons and control an effector. For example, a BMI device designed for human quadriplegic patients successfully used single neuron activity to move a cursor on a computer screen. However, these devices eventually failed. This failure was not due to failure of the microelectrodes, but more likely due to damage to surrounding tissue that results in the formation of a non-conductive glial scar.

The use of nanostructured microelectrode surfaces to mimic the extracellular environment has been previously shown in vitro to positively affect neural survival and decrease glial cell proliferation. In this thesis, we tested whether nanostructured porous silicon would reduce glial activation around the microelectrode compared to smooth silicon. To accomplish this, we first designed a semi-automated process to quantify immunological staining around the microelectrode hole. We then examined the effect of implanting different surfaces for 1, 2, 4 and 6 weeks. Our immunohistochemical quantification process showed that porous surfaces decreased astrocytic up-regulation around the microelectrode insertion site, including less hypertrophied astrocytic cell bodies. Additionally, survival of neurons increased and recruitment of macrophages was

decreased at one week post-insertion. Therefore, nanostructured porous silicon is more compatible with the brain environment than smooth silicon.

In the long term, we hope that implementation of a nanostructured microelectrode surface will lead to a sustainable, chronically implantable microelectrode that can record from every recording site indefinitely. Once this goal has been achieved, BMI devices will be viable alternatives to patients who have lost normal motor function.

1. INTRODUCTION

In the past few decades, recording microelectrodes have been utilized to obtain electrical information directly from neurons to quantify brain activity. Many different types of these recording microelectrodes have been developed for this purpose. The implementation of recording microelectrodes in the human brain holds great promise for therapeutic treatments as well as the interface for a direct Brain-Machine Interface (BMI) (Nicolelis et al., 2003). This interface could restore some level of voluntary interactions for severely paralyzed patients through the manipulation of an external effector, such as a cursor on a computer screen (Hochberg et al., 2006). Although there are less invasive methods for moving a cursor on a screen, the ability to record from populations of single neurons has the potential to allow for finer controls. The existing methods of using eye gaze or electroencephalography (EEG) recordings do not provide as many degrees of freedom for effector control and require all of the individual's attention. For example, the eye gaze methodology requires that the patient look only at the sensing device throughout its use. Implantable BMI technology has the promise to provide an avenue for reconnecting motor areas of the brain to an external effector for use that is more 'unobtrusive' (Hochberg et al., 2006). However, all in vivo human applications involving the use of recording microelectrodes require the ability to chronically record action potentials from ensembles of single neurons indefinitely (Suner et al., 2005).

Unfortunately, long term and sustainable use of recording microelectrodes has not been realized. This failure is hypothesized to be due not to the electrical failure of the devices but instead due to the biological response elicited by the insertion of the

microelectrode. Current studies show loss of discriminable single unit action potentials on the order of days, weeks, or in rare studies, months (Szarowski et al., 2003). For most microelectrode types, the loss of these recordings is not due to failure of the microelectrodes but more likely due to damage to surrounding tissue that results in the formation of non-conductive glial-scar. In this way, the loss of discriminable action potentials is the direct result of the formation of the non-conductive glial scar, or sheath, which electrically isolates the microelectrode from the surrounding tissue.

Our hypothesis is that one aspect of the microelectrode surface that is incompatible with the brain environment is the smooth surface of the implanted microelectrode shaft. Although many biological implants are made smooth to elicit less of a foreign body response, neural tissue is itself nanostructured and therefore this smooth surface many appear more unusual to the brain environment. Since the neural tissue is comprised of many elements that create nanostructured surfaces, such as the microtubule support of the cells in the brain, we propose it is best to implant microelectrode surfaces with nanostructure. The use of nanostructured microelectrode surfaces to mimic the extracellular environment has been shown to positively affect neural survival and decrease glial cell proliferation in vitro (Moxon et al., 2004). This thesis will quantify the affects of nanostructured surfaces to improve microelectrode biocompatibility in vivo.

In the long term, we hope that the implementation of nanostructured microelectrode surfaces will lead to a sustainable, chronically implantable microelectrode that can record from every recording site indefinitely.

2. SPECIFIC AIMS

Specific Aim 1: Design a method to quantify the effects of microelectrode insertion on neuronal tissue.

Specific Aim 2: Quantify the effect of porous silicon surfaces on biocompatibility of microelectrodes in vivo.

3. BACKGROUND INFORMATION

While there is significant information on the brain's response to traumatic brain injury, much less is understood about the immunological and cellular response to insertion of a microelectrode and, more importantly, how this response interferes with single neuron recording. However, this response is complicated and involves many interrelated processes. Therefore, the brain's reaction to the microelectrode is most likely a combination of the body's general immunological response (Ludwig et al., 2006), the specific foreign body response (Anderson, Rodriquez, and Chang, 2008), and the trauma of microelectrode insertion (Zhong and Bellamkonda, 2005); each possibly involving the same cell types via different cellular pathways.

There are two major pathologic states induced by the chronic implantation of arrays of microelectrodes into the brain (Moxon, 1999). The first is a result of the action of inserting the microelectrode. When inserted, the microelectrode passes through the tissue and will damage and tear neuronal and glial processes, thus exposing the extracellular environment to intracellular proteins (Schultz and Willey, 1976). In addition, even if one is careful to miss surface blood vessels, complete insertion of the microelectrode is likely to tear small capillaries, thus damaging the blood brain barrier (BBB) and exposing the extracellular environment of the brain to blood proteins (Schwartz et al., 2006). The exposure of the extracellular environment to both intracellular and blood proteins initiates a cascade of events that can help to remove the damaged tissue and debris and heal the tissue or, if the damage is severe, create a glial

scar that electrically isolates the microelectrode and prevents it from recording single neurons.

The second major effect arises from the continued presence of the microelectrode in the neural tissue, commonly referred to as the foreign-body response (Anderson, Rodriguez, and Chang, 2008). If the brain is subject to a stab wound with a device about the size of a microelectrode, within six months, it will be difficult to identify the location of the wound if the procedure was completed under sterile conditions. The definition of a stab wound, in this instance, is that a device is inserted, then withdrawn, then the dura and skull are replaced over the stab site. However, if the device used to create the stab wound is left in place, a glial scar will form around the device, effectively walling it off from the healthy neural tissue (Liu et al., 1999).

Understanding the biological response to microelectrode insertion is important as the biocompatibility of the microelectrode is directly related to the cellular response of the brain to microelectrode insertion.

To address the issues surrounding the brain's response to microelectrodes, it is first important to understand the different types of cells involved in the immunological response and how this response is naturally regulated. Because this is such an important issue for recording from single neurons, the attempts to minimize this cellular response after microelectrode insertion will also be described. Finally, the challenges of quantifying this response will be introduced through the description of recently developed methods to quantitatively measure the cellular response as a method to better target approaches that mitigate the adverse effects of the response on single neuron recording.

The Cellular Response

There are three main cell types directly involved in the brain's response to injury: microglia, macrophages, and astrocytes—collectively referred to as glia (Fawcett and Asher, 1999). In the event of injury, each of these cell types are up-regulated into their activated state (Seymour and Kipke, 2007). This transformation includes physical changes to cell morphology, expression of different surface proteins that act as signals to other cells, and changes in release of neurotrophic factors (Elkabes, DiCicco-Bloom, and Black, 1996). Damage to neurons, glia, and the BBB initiate this transformation. All three types of cells will be discussed, with special emphasis on their activation process and contribution to the glial scar, the formation of which is likely the primary reason for loss of single neuron recordings. Figure 1 shows a representation of staining specific to these cell types. Two comprehensive reviews: Anderson, Rodriguez, and Chang (2008) and Polikov et al. (2005) are in literature and provide a detailed description of the cellular mechanisms of this response.

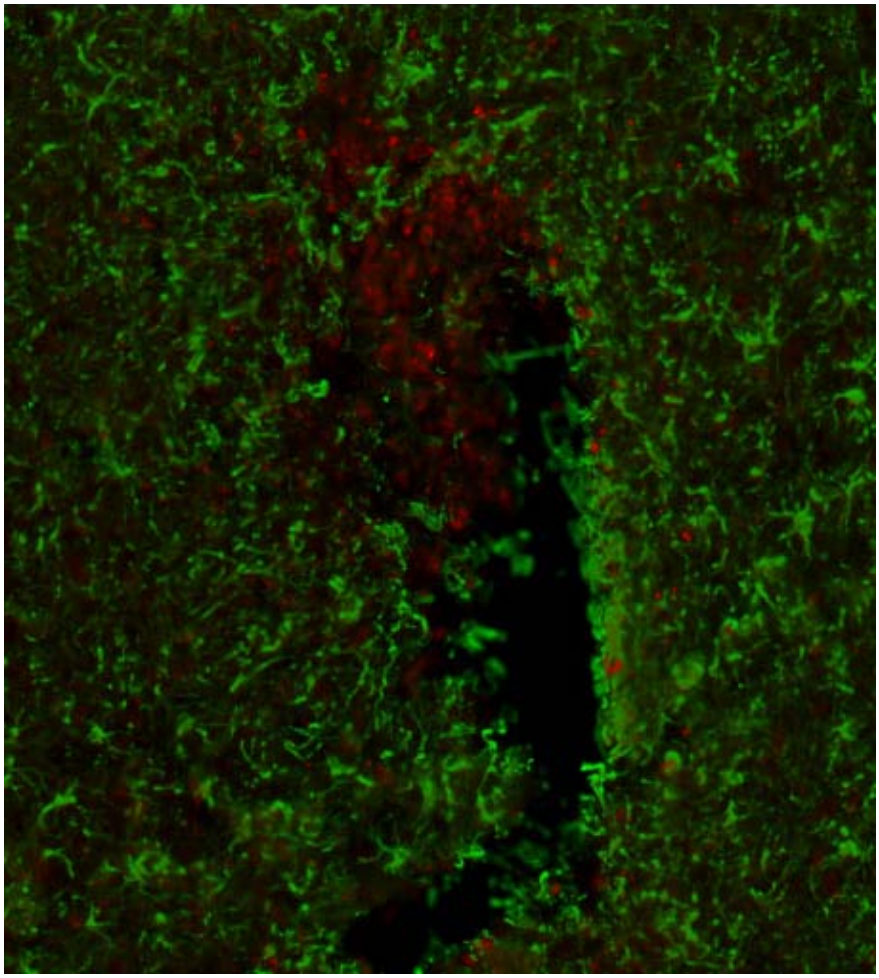

Figure 1: Histological Representation of Astrocytes, Microglia, and Macrophages
This figure is a colorized image depicting the cellular reaction to electrode insertion. Astrocytes are shown in green and macrophages are shown in red. This image was captured at a magnification of 10x.

Microglia are the first of the three cells to become activated in the event of an injury. 5-10% of all glial cells found in the healthy brain are microglia (Ling, 1981). Under healthy brain conditions, the microglia have long, thin processes that are highly branched. In the healthy brain, microglia are the primary defense against pathogens and constitute the initial immune response in the brain. One way microglia destroy foreign pathogens is through the use of cytotoxicity. Additionally, these cells are able to utilize

proteolytic enzymes to dissolve cellular debris. Once dissolved, the remnants can be removed via a variety of processes including phagocytosis (Streit, 1995; Purves et al., 2001). Therefore, microglia serve an important function in the brain.

In response to a traumatic injury to the brain, microglia are activated within 24 hours of the time of injury (Raivich et al., 1997). Intracelluar debris released from damaged cells or blood released from damage to the blood brain barrier triggers microglia to express signals that attract other microglia to migrate to the site of the injury (Elkabes, DiCicco-Bloom, and Black, 1996). These signals also induce proliferation of the microglia surrounding the injury. In this activated state, the microglia morphology changes: the size of the cell body is increased, branching of the processes is reduced, and there is a marked thickening of the distal processes. This results in an 'ameboid' morphology (Giulian et al., 1986).

Activated microglia have both beneficial and detrimental effects for the injured brain; often working through the same cellular signaling mechanisms. For example, one benefit of the activated state to the injured brain is the increased secretion of neurotrophic factors and cytokines by the microglia in order to promote neuronal survival (Elkabes, DiCicco-Bloom, and Black, 1996). There are several important neurotrophic factors that are functionally and structurally related including nerve growth factor (NGF), brain-derived neurotrophic factor (BDNF) and neurotrophin-3 (NT-3) (Wiesmann and de Vos, 2001). These neurotrophins have positive effects on axonal growth and are involved in the development and maintenance of neurons (Moore et al., 2006). Direct secretion of NGF and BDNF by cultured microglia has been demonstrated in vitro (Elkabes, DiCicco-Bloom, and Black, 1996).

Activated microglia secrete cytokines that directly and indirectly regulate the production and release of neurotrophic factors, which can further benefit neuronal survival. For example, activated microglia secrete interleukin-1 (IL-1) and tumor necrosis factor alpha (TNF-α). IL-1 induces astrocytes to release NGF (Woodroofe et al., 1991) and TNF-α, which is also involved in the production of interleukin-10 (IL-10). Through different pathways, IL-10 is inhibitory for the production of TNF-α or produces a positive feedback loop that increases the production of TNF-α (Sheng et al., 1995). This same relationship is observed between IL-6 and NGF (Kossmann et al., 1995). Additionally, the activation of microglia is observed to precede asytrocyte activation and therefore the signaling pathways both these two cell types are interrelated and possibly causal (Babcock et al., 2003). Overall, microglia are involved in initiating a complex chemical signaling cascade that can increase the production of neurotrophic factors through regulation of cytokines and their influence on astrocytes.

Through these same mechanisms, the activated microglia can have detrimental effects on neuronal survival because of the damage elicited from inflammation and high concentrations of neurotropic factors. Microglia are a potent source of monocyte chemo-attractant protein (MCP-1): a chemokine. MCP-1 molecules recruit macrophages and activate microglia creating an inflammatory state. In addition, cytokines, such as IL-1, released by microglia can contribute to the inflammatory state by stimulating astrocytes to become reactive (Giulian et al., 1994). In addition, both microglia and TNF-α can stimulate production of nitric oxide (NO) (Sheng et al., 1995) which has a cytotoxic effect on neurons.(Minghetti and Levi, 1998; Fitch and Silver, 1997). These studies suggest that the same mechanisms that can aid in the repair of neural tissue, can, if

damage is severe, create an inflammatory state that further damages nearby, otherwise healthy, neurons.

Some activation of microglia following microelectrode insertion is clearly beneficial to clear debris from torn and damaged neurons and secrete neurotrophins to aid in the survival of local cells damaged by microelectrode insertion (Nakajima et al., 2001). However, excessive damage to brain tissue induces over-proliferation of microglia and their signaling molecules, leading to inflammation and subsequent cell death. When considering the insertion of microelectrodes, the damage of insertion accompanied by the continued presence of the microelectrode shaft is likely to be sufficient enough to lead to excessive activation of microglia. The optimal situation would be to allow for some activation of microglia, sufficient to induce their beneficial effects, without overproduction, inflammation, and excessive damage. Unfortunately, little is known about where the effects of microglia shift from being beneficial to detrimental and it is likely this threshold exhibits biological fluctuations depending on many variable biological factors. Therefore, microglia will require more intensive study to be better understood, and eventually manipulated, to aid in the long term success of chronically implanted microelectrodes.

The next cell type involved in the brain's response to the microelectrode insertion is the macrophage. Macrophages are not normally found in neural tissue but exist within the vascular system. When blood vessels within the brain are severed, monocytes from the blood are recruited into the neural tissue via the break in the BBB and are induced into morphological changes to become macrophages (Fitch and Silver, 1997). Other components located within the vascular system, such as the complement system, also are

indicated to respond to the break in the BBB but discussion of these immunological compounds is beyond the scope of this report (Hortbit, 2004). It is important to note that although their origins are different, the up-regulated microglia inherent to the brain and the macrophages recruited through this break are morphologically indistinguishable.

The effects of macrophages are confounding following microelectrode insertion. This is because their presence is necessary following severe damage in order to scavenge extensive cellular debris but their presence can also induce inflammation which further damages neurons and further induces cascades that increase the up-regulation of microglia (as discussed above) and astrocytes (as will be discussed below).

Similar to microglia, macrophages are responsible for dissolving cellular debris by secreting protolytic enzymes and removing the debris via phagocytotsis (Fitch et al., 1999; Biran et al., 2005). They also fuse together to form foreign body giant cells, which causes extreme inflammation (McNally and Anderson, 2002). This excessive inflammation due the foreign body giant cells can lead to cavitations at the site of a gross injury (Fitch et al., 1999). Staining specific to macrophages and microglia is shown in Figure 2.

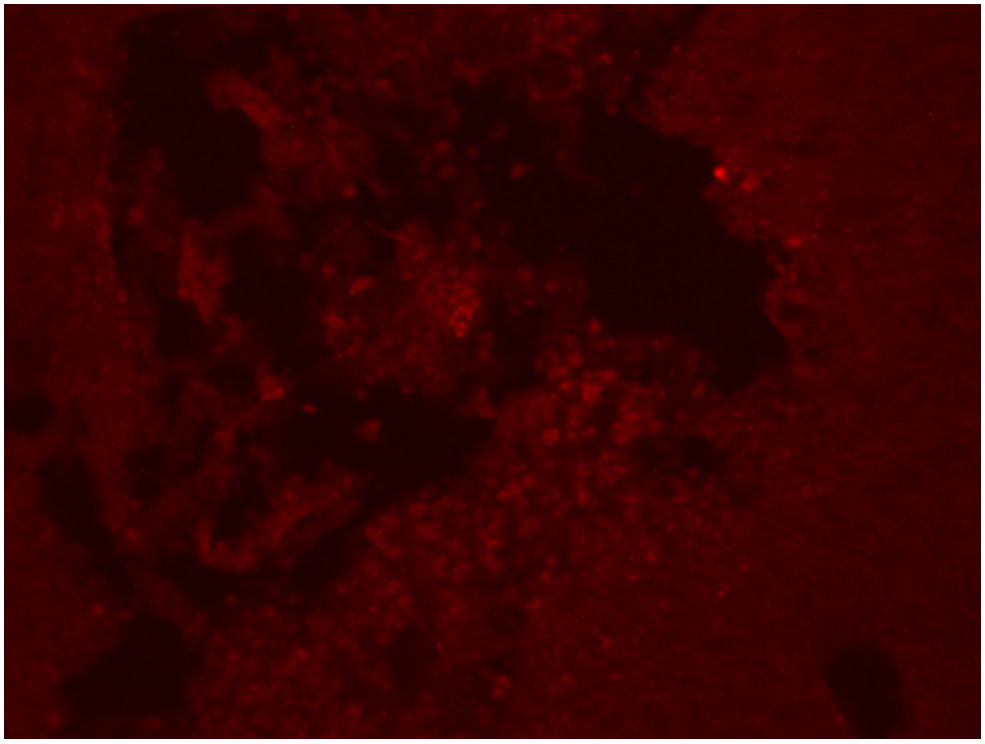

Figure 2: Microglia and Macrophages Surrounding Microelectrode Insertion
This figure shows the histological identification of microglia and macrophages surrounding the microelectrode track. This image was captured at a magnification of 10x.

Similar to the conclusion regarding microglia, since insertion of a microelectrode must damage the BBB, some proliferation of macrophages to clean up the damage is necessary. However, this proliferation must be managed and eventually down-regulated to allow the microelectrodes to remain in contact with healthy neurons for long-term, chronic recording.

The final important cell type in the brain's response to microelectrode insertion is the astrocyte. Astrocytes constitute 30-65% of glial cells found in the healthy brain (Nathaniel and Nathaniel, 1981). In the healthy brain, astrocytes have many widespread cellular processes and perform multiple beneficial functions. Astrocytes provide mechanical support to neurons throughout their lifespan and provide growth cues to

developing neurons. Astrocytes also assist the transfer of nutrients across the BBB and take part in regulating the chemical environment required for healthy neuronal function (Araque et al., 1999). Astrocytes in the healthy state are shown in Figure 3.

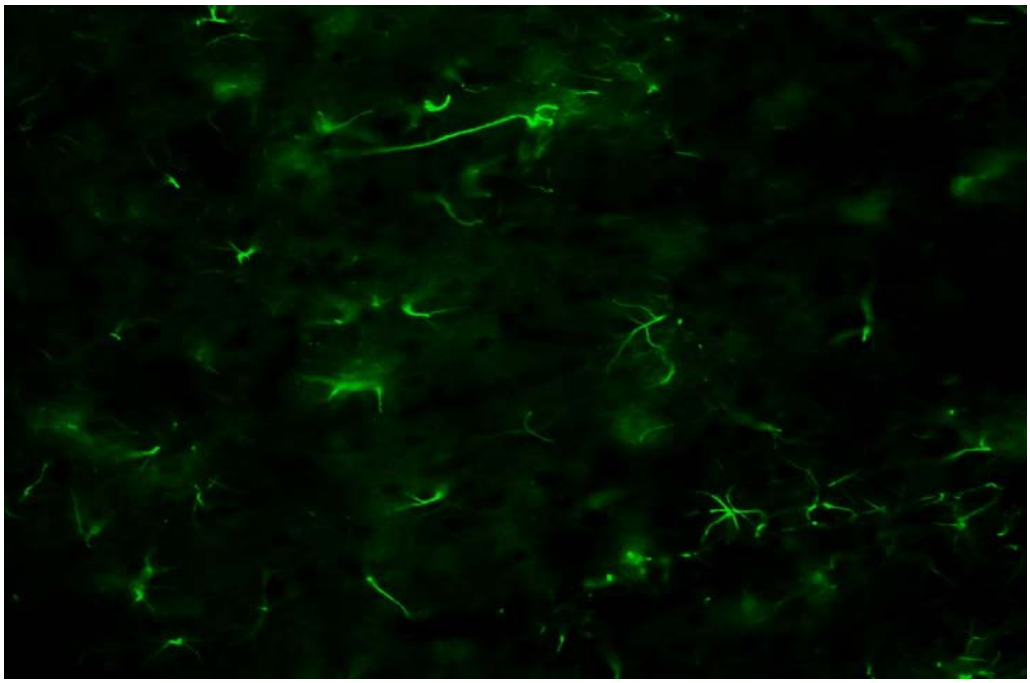

Figure 3: Astrocytes in the Healthy Brain
This figure shows the histological identification of astrocytes in the healthy brain. This image was captured at a magnification of 10x.

Activation of astrocytes takes place within the first week of injury—in this case microelectrode insertion. Immediately after activation, the astrocytes proliferate and migrate to the site of injury (Landis, 1994; Raivich et al., 1997). In this state, astrocytes are also known as reactive astrocytes (Klaver and Caplan, 2007). A visual representation of astrocytic up-regulation is shown in Figure 4.

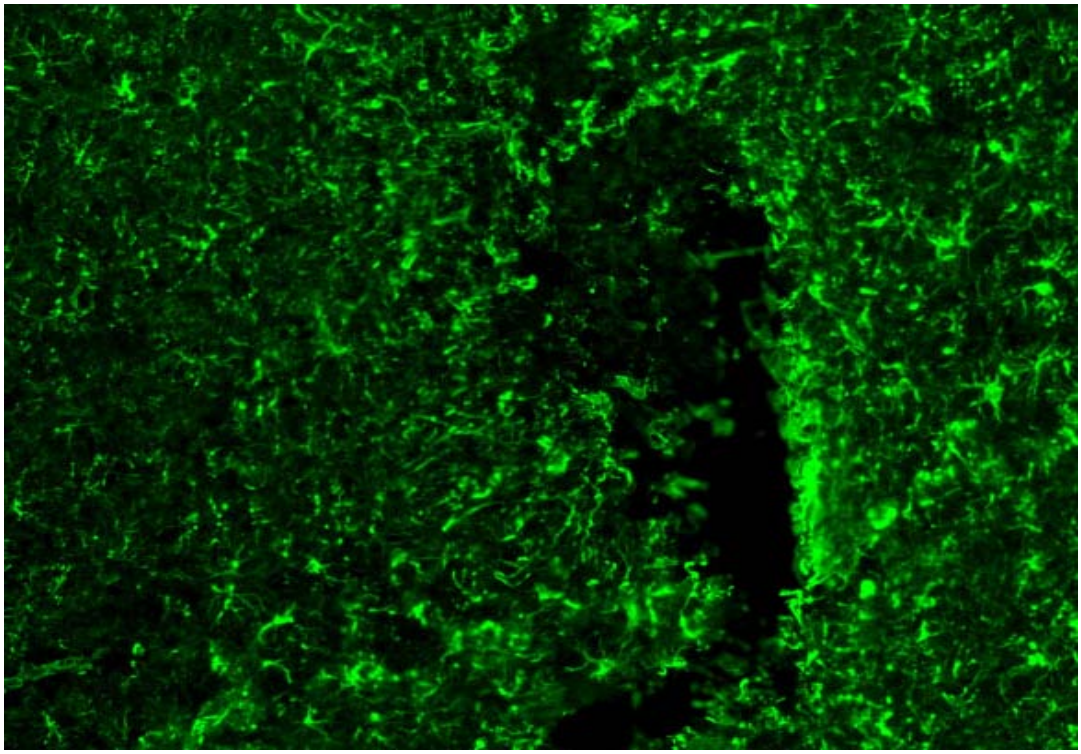

Figure 4: Astrocytes Surrounding Microelectrode Insertion
This figure shows the histological identification of astrocytes surrounding the microelectrode track. This image was captured at a magnification of 10x.

The primary beneficial effect of reactive astrocytes is to aid in the production of NGF, which helps repair damaged neurons (Goss et al., 1998). However, reactive astrocytes have numerous detrimental effects to full tissue recovery which can interfere with the ability of microelectrodes to record from single neurons. Astrocytes have been shown to create a physical barrier between healthy and damaged tissue which creates an inhibitory environment for neurite extension (Raivich et al., 1997). This same physical barrier can electrically and physically separate the microelectrode from healthy cells (Turner et al., 1999) preventing neuronal recordings. Therefore, similar to microglia and macrophages, some activation of glia is useful to support damaged cells, but, ultimately,

the goal is to control this activation and have the tissue return to its normal, resting state following the insertion of the microelectrode.

Unfortunately, the exact time course of the cellular up-regulation following microelectrode insertion is not well understood and requires more study. The next section will examine how to monitor the time course of immunological events after microelectrode insertion using immunohistochemistry. The approaches that have been used to minimize the immunological response will then be discussed with regards to their attempts to improve neuronal recordings. Finally, methods to monitor the effectiveness of neuronal recordings will be discussed.

Measuring the Immunological Response

Knowledge of the cellular response to microelectrode insertion does not immediately lead to a solution for successful implantation of the microelectrodes for chronically sustainable recordings. While some of the factors that contribute to this scar (size of the device inserted, speed of insertion, etc) and mechanisms of scar formation, (recruitment of macrophages, activation of microglia, etc.) have been well studied (Klaver and Caplan, 2007), the relationship between single neuron recording and glial scar formation are less well understood.

The effects of microelectrode insertion outlined above interact in such a way that despite the fact that the loss of recording occurs months after implantation, processes initiated during the acute phase of the response persist and contribute to the eventual encapsulation of the microelectrode. Traumatic brain injury research has shown that

mechanical trauma can initiate progressive degeneration that continues long after the traumatic event (Raghupathi et al., 2000).

The ability to understand the brain's response to microelectrode insertion on the cellular level is important for directing interventions to optimize the ability to obtain neuronal recordings indefinitely. Because the cells involved in the reaction to the inserted microelectrode—in their activated states—express novel proteins on their surface, immunohistochemistry can be used to label cells that express these proteins and the amount of labeled tissue can be quantified. Therefore, utilizing immunohistochemistry to classify and quantify the cellular response is an integral part of evaluating response reduction.

Proteins that are specific to the previously discussed cells of interested have long been identified and studied in the literature (Leung et al., 2008). During conventional immunohistochemical analysis, these proteins are associated with a primary antibody that will bind to the protein of interest (refer to Table 1). Once the primary antibody has bound to the protein, a second antibody tagged with a detection agent is then added to bind to the primary antibody. This allows for visualization under a microscope for further analysis (Leung et al., 2008).

In order to prepare brain tissue for immunohistochemical analysis, the animal is usually perused transcardially—with a needle through the heart. The animal is first perfused with biological saline to flush the blood out of the tissue and then paraformaldehyde to fix the tissue. In some cases, analysis will be done on fresh tissue instead of fixed tissue (Kerns et al., 1992). Then, the entire animal is placed in the fridge for 1-2 days, following which time the brain is dissected. This period of time is not

always utilized for other immunohistochemical applications, but is important for studying microelectrode insertion as it gives the tissue time to fix and makes it less likely that tissue will be unintentionally removed by microelectrode cap removal. At this point, the tissue is often ”blocked” to remove unwanted sections of the brain from the area of interest. Finally, the brain is placed in a surcrose solution for several days (Porada et al., 2000).

After the brain has been equilibrated in the sucrose solution, the tissue is carefully frozen and sliced to a thickness between 10 microns and 30 microns. Thinner tissue slices allow more of the tissue to be visualized but are harder to manipulate without damaging the tissue. The tissue can be sliced using a variety of tools, including the cryostat, microtome, and vibratome (Leung et al., 2008; Shain et al., 2003). Once the tissue is sliced, it can be directly mounted to a slide for staining or it can be floated in phosphate buffered saline, stained, and then mounted onto a slide (Stensaas and Stensaas, 1978). Floating samples yield better staining because the stains can penetrate both sides of the tissue and, when transferred to a slide, bubbles underneath the tissue are less likely to form. However, mounting cut tissue directly to slides makes the tissue more likely to rip and, more importantly for microelectrode-tissue response analysis, it is easier to monitor the relative depth of the tissue slice in the brain for later three dimensional data reconstructions.

In the past, the stain used to tag the protein of interest was a monochromatic stain, which only allowed one cell type to be viewed on a given tissue slice. However, newer stains utilize fluorescence, allowing antibodies that fluoresce under different wavelengths of light to be used simultaneously on the same tissue sample. This allows for the labeling

of multiple cells on the same slice of tissue as well as a better image of the proximity of different cells types to one another since the images can be overlaid with imaging software to view all cell types simultaneously (Doroski, Brink, and Temenoff, 2007).

In order to better understand the brain's response to microelectrode insertion, there are primary antibodies that stain the cells of interest as shown in Table 1. Examining tissue with and without microelectrode insertion with these types of stains can be useful in studying the effect of microelectrode insertion on the presence and proliferation of the immunological cells of interest.

Table 1: Primary Antibodies To Identify Cells of Interest
This table lists the common primary antibodies that bind to the cells of interest to the microelectrode insertion reaction. This binding is due to the unique expression of proteins on the surface and within these cells.

Cells of Interest	**Primary Antibody**
Microglia	ED1 (CD68)
Macrophages	ED1 (CD68)
Astrocytes	GFAP
Neuron Cell body Cell Process	 NeuN MAP2

Most preliminary studies that use immunohistochemistry to better understand the effects of microelectrode insertion into the brain are qualitative (Cui et al.,2003; Turner et al., 1998). However, there is an entire field of stereology that describes methods for counting or measuring the density of cell types and can aid in making quantitative measures of the effect and time course of cellular response to microelectrode insertion into the brain. Unfortunately, limited studies have been done to date utilizing these quantitative techniques (Biran et al., 2005). Moreover, the attempts to quantify the

morphological changes to up-regulated cells have not been well studied (Edell et al., 1992). This information is critical to designing appropriate interventions that minimize the immunological reaction to microelectrode insertion in order to maintain healthy tissue around the microelectrode for sustainable, long-term recordings.

Minimizing the Cellular Response to Microelectrode Insertion

Several investigators have studied the effects of microelectrode insertion into the brain in the attempt to develop methods to minimize negative effects on the tissue from insertion (He, McConnell, and Bellamkonda, 2006). Further research should be done in this area because of the need to record for long periods of time from large numbers of single neurons simultaneously in vivo. The ability to complete these recordings is imperative to further our understanding of the functioning of the brain and to improve the success of potential clinical applications (He, McConnell, and Bellamkonda, 2006). The methods utilized to attempt to minimize deterioration of the tissue around the inserted microelectrode include optimizing the geometry of the microelectrode, modifying the surface structure, and coating the surfaces with bioactive molecules to control the cellular response. Each of these approaches will be examined next.

Investigators have explored the influence of microelectrode shapes, especially at the tip of the microelectrode on the brain's reaction to microelectrode insertion. However, well controlled studies were not performed until the last half decade. Szarowski et al. (2003) performed a comprehensive study on the long-term success of a variety of surface modifications and their affect on the chronic tissue reaction to the microelectrode. This

group studied size, surface texture, cross sectional shape, tip geometry, and insertion technique to determine the effects of these aspects on the short and long term reaction to microelectrode insertion. Microelectrodes with either a 2500 μm^2, 10,000 μm^2, or 16,900 μm^2 cross sectional area and either trapezoidal, square, or ellipsoidal cross sectional geometries were compared against one another. Smooth surface textures or micrometer rough surface textures, blade or rounded tip geometries, and slow and fast insertion techniques were also compared. Using qualitative estimates of the amount of GFAP and ED-1 staining, they concluded that the size of the microelectrode had an effect on cellular up-regulation one week after insertion, but this effect was not evident after six weeks. However, more quantitative measures are necessary to fully explore these findings and their implications.

Recent in vitro studies are beginning to suggest that changes in surface structure on the nano scale level can have an important effect on neurons and glia. McKenzie et al. (2004) studied the effect of carbon nanofiber coatings on astrocyte proliferation in-vitro. These coatings were either 60 or 200 nm and with either high or low surface energy. These results showed that microelectrode tips coated with fibers of smaller diameter and higher surface energy lead to a decrease in astrocytic adhesion. Since these cells are one of the primary cells believed to be involved in the encapsulation and isolation of the microelectrode in vivo, the group concluded that it may be possible to decrease the glial encapsulation of the microelectrode by manipulating the surface structure of the microelectrodes at the nano-scale (McKenzie et al., 2004).

The effects of modifying the surface of the microelectrode with surface polymers have also been studied (Buchko et al., 2001; Xiao et al., 2006). Electrochemical

polymerization was used to deposit both polymer and bioactive molecules onto the surface of microelectrodes to improve the signal conduction at the recording site surface and to attract neurons (Cui et al., 2001; Kim et al., 2003; Xiao et al., 2006). These devices were tested both in vitro and acutely in vivo. These experiments were able to show high levels of function as well as preferential neuronal growth on the surface. Chronic testing showed that this approach could produce stable neural recordings at some sites after one week, following which time the recordings were lost (Cui et al., 2003). Surface coatings such as silk-like polymer having fibronectin fragments (SLPF) and nonapeptide (CDPGYIGSR) have also been found to increase neuronal growth and decrease glial proliferation (Cui et al., 2001). Other surface coating such as fibronectin and laminin have also been used on the surface of microelectrodes as they are extracellular matrix proteins that help guide cell movement and facilitate cell adhesion (Hynd et al., 2007; Stauffer and Cui, 2006). Therefore, conducting polymers may provide improved interfaces between microelectrodes and neural tissue but more work is required to better understand this interface and how conducting polymers can improve neuronal recordings chronically.

The effect of surface structure was also studied comparing mesostructured porous silicon (PS) to nanostructured porous silicon (PS) as novel surface coatings for ceramic-based microelectrodes (Moxon et al., 2004). In vitro studies showed that neurons preferred the nanostructured surface by extending significantly more neurites while glial cells avoided the nanostructured surfaces, suggesting that this surface may be useful for targeting appropriate cell types in vivo. Subsequent in vivo studies showed that microelectrodes coated with nanostructured porous silicon could be used to record single

neurons. More studies over longer time periods are necessary to determine if these surfaces have a useful effect for improving long-term biocompatibility.

There are generally three approaches to using bioactive molecules to improve microelectrode recording: delivering drugs via microfluidcs, systemic injection of drugs to minimize the immunological response, and attaching biomolecules to the surface through some type of chemical bond (conjugation). Some investigators have attempted to incorporate microfluidics to deliver novel drugs to the insertion site in order to attenuate the biological response to microelectrode insertion (Retterer et al., 2008). Researchers studying microfluidics have incorporated drug delivery channels into the microelectrode tips. In order to make these fluid channels beneficial though, fabrication technique must be utilized that can incorporate these channels without greatly increasing the size of the microelectrode tip. The groups who have been successful in fabricating microelectrodes with incorporated microfludics channels (Retterer et al., 2004; Cheung et al.,2003) found that it was possible to deliver labeled compounds of similar molecular weight to active drugs into tissue like materials in-vitro as well as in-vivo over short time periods. However, since no long term studies of these microfludics have been completed, there is no way to know if the same cellular processes that physically isolate the microelectrode from the normal cellular environment will occlude these channels and render them useless.

Koyoma et al. investigated the effects of BQ788 on reactive astrocytes. BQ788 is an endothelin ET_B receptor antagonist. Endothelin molecules have been shown to regulate the function of astrocytes through DNA synthesis. Reactive astrocytes and activated microglia are the main cells that express the ET_B receptor. Injury was induced in male

rats by a unilateral stab wound using a razor blade. BQ788 was administered by continuous infusion and showed a significant decrease in the GFAP staining at two weeks post injury. However, this ET_B receptor antagonist showed an increase in the number of microglia. Therefore, endothelin has shown potential to be used in future experiments, though one must investigate the effects of this receptor antagonist for a longer time period. The effects of this receptor antagonist also need to be investigated in vivo.

Tomobe et al. (1996) investigated the effect of anti-coagulation factor protein S on activated astrocytes. Protien S is a plasma protein expressed in cultured glial cells. Injury was induced by scratching cultured rat astrocytes in vitro. Protein S activity was measured by using a functional clotting assay in the presence of serum and in the absence of serum. At a concentration of 100 nM, Protein S suppressed the proliferation of reactive astrocytes by 50%. At a concentration of 300nM, it suppressed the proliferation by 90%. The mRNA expression of Protein S was also investigated and a marked increase in the concentration was observed 15 hours after injury. This up-regulation of Protein S mRNA expression after injury suggests that Protein S may be involved in regulation astrocyte proliferation after injury.

In another set of experiment, tumor necrosis factor-β1 (TNF-β1) was administered to the cultured astrocytes since TNF-β1 is known to be a strong inhibitor of astrocyte proliferation. Cell growth was assessed by incorporating [^{3}H] thymidine and bromodeoxyuridine BrdU in cultured astrocytes for 24 hours. Reactive astrocytes were reduced to 50% of control level when TGF-β1 was administered at a concentration of 20 ng/ml. Protein S had a comparable effect on the astrocytes at a concentration of 100 nM.

These interventions clearly show an inhibitory effect on astrocyte proliferation and they should be investigated in vivo to fully understand their potential.

Steroids also have the potential to improve neuronal recordings in vivo because of their ability to reduce inflammation. The effects of dexamethasone, an anti-inflammatory synthetic glucocorticoid was investigated on astrocytes (Spataro et al., 2004; Zhong and Bellamkonda, 2007). A single dose of dexamethasone was administered to animals after surgical implant of microelectrodes into the brain. The animals were sacrificed at week 1 and week 6 and the brain sections were stained for GFAP, CD11b and laminin. Reactive astrocytes were observed around the device shank. Interior to the layer of reactive astrocytes, activated microglia was observed. The reactive astrocytes transformed into a compact sheath by week 6. The astrocyte layer extended to diameter of 400 micrometer from the device shank. Laminin staining and CD11b staining was observed to be minimum. Since a single dose of dexamethasone did reduce the glial response to an extent, dexamethasone was injected daily for one week. At six weeks, a compact sheath of astrocytes was observed but was poorly developed and showed no significant hypertrophied morphology. However, there was increased laminin and $CD11^{+}$ staining. These studies suggest that dexamethasone has the potential to regulate astrocyte proliferation but additional side effects of this treatment should be studied. Dexamethasone, along with other neurotrophic factors, can be used in drug delivering systems at the site of microelectrode implantation to curtail the problem of glial scarring (Kim and Martin, 2006).

Other groups have proposed to immobilize biomolecules on their microelectrodes to mediate the cellular response. Azemi et al., (2008) immobilized L1 molecules—which

are neuronal adhesions molecules indicated in the neuronal pathways of mobility and growth—on laminin constructs placed around the microelectrode. The group was successful in promoting the pathways involved with the L1 molecule surrounding the inserted microelectrode and therefore showed better biocompatibility of this surface compared to control groups (Azemi et al., 2008). Other compounds, such as BDNF (Jun et al., 2008) and polymer poly(3,4-ethylenedioxythiophene – PEDOT) (Richardson-Burns et al., 2007), have also been immobilized on microelectrode constructs and shown, in vitro, to improve neuronal proliferation around the microelectrode material.

Another compound studied for the use of mitigating neuronal injury is Poloxamer-188. Poloxamer-188 is a water-soluable, non-ionic surfactant first studied for use in mitigating traumatic brain injury. Due to its surfactant properties, it is believed to work by sealing damaged membranes, thus preventing contamination of the extracellular space by intracellular proteins and promoting cell survival (Serbest, Horwitz, and Barbee, 2005; Serbest et al., 2006). However, there is no work in literature of applying this compound to implanted microelectrodes.

Evaluating the Success of Response Reduction

The most important practical indicator of successful reduction of the cellular response to microelectrode insertion is the ability to continue to obtain consistent recordings of single neuron action potentials over a chronic period of time.

The scar tissue that begins to surround the microelectrode following insertion electrically isolates the microelectrode from the brain environment. Therefore, as greater

amounts of scar tissue begin to build up, it is harder to discern single actions potentials from the background noise (Winter, Cogan, and Rizzo, 2007). These single action potentials are the signal of interest and therefore, as the ability to record these single action potentials decreases, so do the ability to use the information for different applications.

Some groups have achieved chronic recordings from current implantation techniques. Porada et al. (2000) were able to record discernable action potentials from the brain of a monkey for more than a year. Importantly, they quantified their recording stability through four measures: "spike shape, spike train autocorrelograms, spike frequency, and range of peak amplitudes."

Spike shape was evaluated by a vector made from three spike characteristics. The first characteristic was the amplitude of the first phase of the spike, the second characteristic was the amplitude ratio comparing the first and second phases of the spike, and the third characteristic was 'inter-peak-interval' of the spike. These three components yielded a numerical vector that could be normalized and used to compare the spike shape between different recording sessions. These types of quantitative measures are useful for comparing results across groups. (Porada et al., 2000).

Another group of investigators attempted to quantify the effect of various cellular foreign body response components through the classification of impedance normalized to saline (Merrill and Tresco, 2005). The concept underlying this measurement is that as the glial scar builds up, the buildup increases the impedance between the recording site and the tissue. Therefore, impedance should be inversely correlated with the quality of the recording, although this has never been shown. In fact, most studies of neural recordings

that measured impedance found no correlation between the quality of the recording and the microelectrode impedance. However, in vitro, Merrill and Tresco (2005) demonstrated that cellular adhesion to the recording site surface yielded changes in the impedance varying from 20% to 80% and this change was shown to persist for a period of weeks. However, this change in impedance was not shown, in vitro, to negatively affect the ability to record (Merrill and Tresco, 2005). Therefore, it is not clear that this change in impedance will address the quality of the recording.

4. OVERVIEW OF EXPERIMENTATION

Adult, male, Long-Evans rats were anaesthetized with Nembutal and implanted with microelectrodes into the somatosensory cortex (see Microelectrodes, below). Following deep anaesthization, the animals were implanted bilaterally with microelectrodes into the somatosensory cortex (see Implantation of Microelectrodes, below). The exposed brain tissue was protected with a coating of agar gel and the microelectrodes were secured to the skull with dental cement. The incision was then closed with surgical staples and the rat was allowed to recover (see Implantation of Microelectrodes, below).

At one, two, four, or six weeks following implantation, the rats were euthanized with an overdose of Nembutal and perfused transcardially with phosphate buffered saline (PBS) followed by 4% paraformaldehyde. Carcasses were then placed in the refrigerator for two days and dissected on the third day to remove the brain and block the tissue. Tissue samples were then placed in 30% sucrose solution for a three day equilibration period and subsequently sectioned on a vibratome into 30 micron sections (see Perfusion and Tissue Processing, below). Sections were immediately mounted onto slides, which were ringed with rubber cement and treated with antibodies for staining (see Histology, below).

Once the tissue samples were treated with staining antibodies, two quantification methods were applied. Samples stained for macrophages and neuron cell bodies utilized a cell counting technique to quantify cellular response to microelectrode insertion (see Counting Method, below) and samples stained for astrocytes were analyzed with an intensity of stain quantification to study cellular response (see Intensity Method, below).

5. MATERIALS AND METHODS

Microelectrode Fabrication

Prior work from this lab has created a method for inducing porosity on the microelectrode surface. The porous silicon coating of our microelectrodes is fabricated via photoelectric etching. This method is beneficial because it offers several process variables that allow for control of pore formation and morphology.

In order to control pore formation and morphology, a variety of factors are varied including: 1) anodic current density, 2) HF concentration, 3) choice and concentration of substrate dopant, 4) illumination wavelength, and 5) direction of incidence.

In preliminary studies, ten primary samples were studied in vitro to determine optimal electrical, mechanical, and biological variations. Samples included n- and p-types Silicon wafers and dopants were either Arsenic, Phosophorous, and Boron. Preliminary data showed that only three samples were of sufficient porosity (>70%) and further in vitro analysis was done on these three samples.

Following cell culture analysis on microelectrode surfaces, type seven was the most successful and is therefore the type of microelectrode surface utilized for this experiment. Type seven surfaces are characterized as having significant porosity with deep pores. The deep porosity can be seen in the three dimensional image shown in Figure 5. Figure 6 is a visual representation of the entire electrode shaft completed through this process.

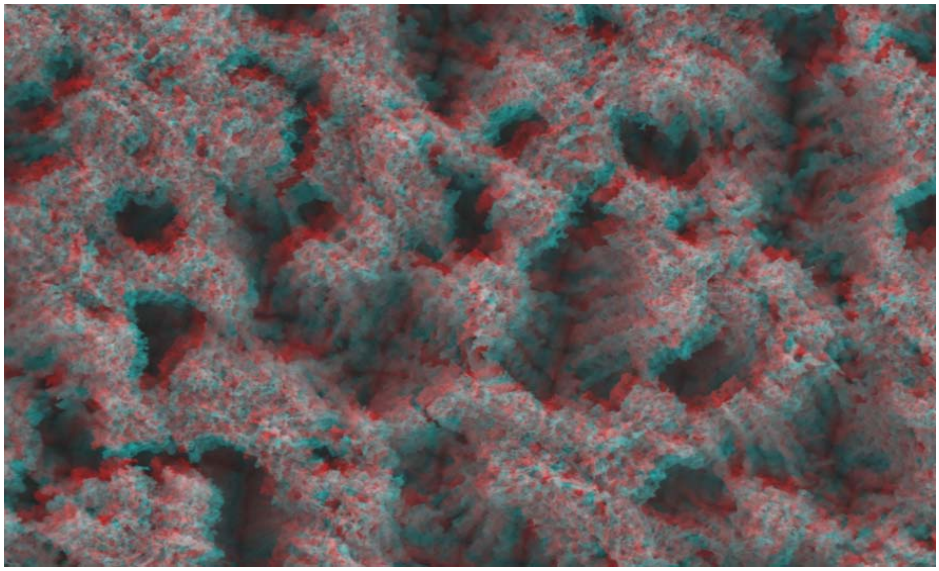

Figure 5: Three Dimensional Representation of Surface Porosity

Previous work done in this lab obtained this three dimensional image showing the depth of pores in the porous silicon samples implanted for this thesis. 3-D glasses are required to see this image clearly.

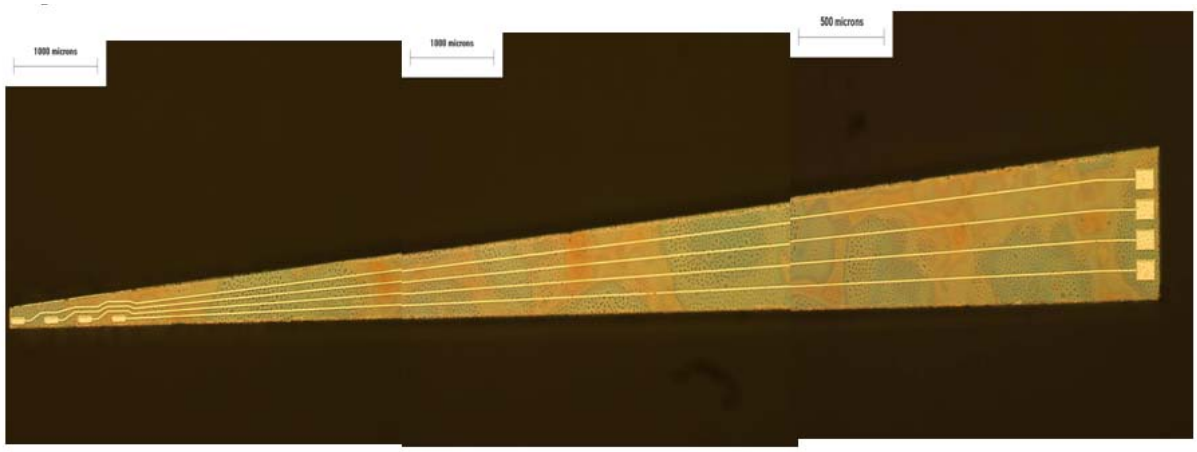

Figure 6: SEM Image of Microelectrode Shaft

Previous work done in this lab obtained this composite 50x magnification images of a diced silicon-based microelectrode with porous silicon coating. Note: the scale bars indicate 1000µm or 1.0mm. Although the same process was used to make this electrode shaft, larger wafers were implanted for this thesis.

Implantation of Microelectrodes

All in vivo surgical procedures were performed utilizing sterile techniques approved by the Drexel University Institutional Animal Care and Use Committee (IACUC). To prepare the adult, male, Long-Evans rats for surgery, rats were anaesthetized with a weight adjusted amount of intraparitenial Nembutal. The rat's heads were shaved and the area was disinfected with an alcohol swab followed by a butadiene swab.

After full anaesthetization was observed, rats were placed on the stereotax, an incision was made to expose the skull, and the skull was centered on the stereotax to bregma. Holes were drilled into the skull at (0, +-3.5), (-3,+-2), and (-5.5, +-4.5) in the anterior/posterior and lateral directions and the microelectrodes were inserted via a tool mounted on the sterotax. The microelectrode was cleaned prior to insertion with a sonicating solution of water followed by a sonicating solution of sterile alcohol. Following this sterilization procedure, the microelectrode was dried with compressed air and subsequently inserted.

Holes in the skull were then filled with agar gel to protect the exposed brain tissue and the microelectrodes were secured to the skull with dental cement. The incision was then closed with surgical staples and the rat was allowed to recover from anesthesia in a heated environment. Rats were each monitored frequently until they fully recovered from anesthesia, and then once per day for the remainder of the study. Seven rats were implanted with six independent mock microelectrode tips each (some related to other studies) for experimentation for this thesis.

Perfusion and Tissue Processing

At one week, two weeks, four weeks, or six weeks following implantation, the rats were euthanized with an overdose of Nembutal or Euthasol and then perfused transcardially with 0.5 L of ice cold PBS followed by 0.5 L of ice cold 4% paraformadelhyde. After perfusion was complete, the carcasses were placed in the refrigerator for two days to allow the tissue to fully absorb the fixants. Additionally, this period of time allows the tissue to solidify to minimize tissue tearing during the removal of the microelectrode. Following this time period, the brains were dissected and blocked to separate microelectrode holes and placed in 30% sucrose solution to equilibrate for three to five days.

Following the equilibration period, the tissue was sliced using a vibratome into 30 µm sections. These sections were collected serially in four groups and mounted onto slides.

Histology

After sections were mounted onto the slides, the slides were then ringed with rubber cement to create wells and treated with antibodies to stain for macrophages, neuron cell bodies, neuron filaments, astrocytes. Group one received ED1 and GFAP to stain for macrophages and astrocytes, group two received NeuN and GFAP to stain for neuron cell bodies and astroyctes, and group three received MAP2 to stain for neuron

filaments. The final group received a nissel stain, to mark all cells and provide as a comparative control.

To prepare tissue for staining, the sections were washed in PBS and then blocked with goat serum. The primary antibody was then applied overnight at a 1:1000 dilution.

Following the primary antibody incubation period, the tissue was washed in PBS and incubated in the secondary antibody for two hours at a 1:100 dilution. The tissue was then washed again and coversliped with Vectashield to help preserve tissue and stain quality.

Counting Method

Once the tissue had been stained, macrophages and neuron cell bodies were quantified utilizing a counting method. Utilizing a fluorescence microscope, four images were captured of each section. The center of the microelectrode hole was used to visually create an axis so that each of the four images captures a unique quarter of the microelectrode hole and the surrounding tissue.

After the images were captured, our unique MATLAB rountine was used to define the radial area 50 μm from the edge of the hole and 150 μm from the edge of the hole. The program was then used to randomly select 15% of the tissue in each of these two areas and cells were manually counted in these representative areas. As the sampling is random, if a larger proportion of the tissue needs to be sampled, the procedure can be repeated to sample more of the tissue. These data were then used to compare cellular

proliferation with distance from the microelectrode site in a paired t-test or ANOVA format.

Intensity Method

After the tissue was stained, astrocyte response to microelectrode insertion was quantified utilizing an intensity method. Utilizing a fluorescence microscope, four images were captured of each section. The center of the microelectrode hole was used to visually create an axis so that each of the four images captures a unique quarter of the microelectrode hole and the surrounding tissue. Equal exposure times were utilized for all images captured to equalize the amounts of background staining captured.

After the images were captured, background staining was removed by calculating the intensity of staining in control tissue and subtracting this level of intensity from all images captured. Then, our unique MATLAB protocol was used to draw four horizontal lines. The edge of the microelectrode tract (empty space) was manually defined by the program operator from visual inspection of the intensity profile. After the lines were drawn, MATLAB determined the intensity of staining at each pixel on the line. These data were then used to compare the amount of astrocyte up-regulation compared with distance from the injury site. This method is discussed in depth in the design component section.

6. DESIGN COMPONENT

Statement of Statistical Challenge

Understanding astrocytic up-regulation is important for quantifying tissue response to implanted microelectrodes as well as to attempting to improve biocompatibility of the implanted microelectrodes, but quantifying this response is difficult. Although cell counting and the related statistical methodologies are frequently utilized following immunohistochemical treatment of tissue, this is not an appropriate approach for quantifying astrocytic cell response. Primarily, counting these cells is difficult because the GFAP stain labels the processes of the astrocyte as well as the cell body and therefore discriminating one cell from another is difficult. Also, even if it was possible to easily count cells in this methodology, cell counts would not include information regarding the hypertrophied nature of upregulated cells. Therefore, a method is required which incorporates quantification of both cells present as well as their hypertrophied character.

Statistical Analysis Protocol

Our approach to GFAP quantification was adapted from the work done by Biran et al. (2005). This approach utilizes a line intensity analysis over multiple horizontal lines of an image of the tissue surrounding the inserted microelectrode. Due to the fact that our lab did not have access to the advanced statistical and image software utilized by Biran et

al., we designed a unique MATLAB routine to generate the line intensity profiles from our images. See Figure 7, below, for a visual representation of the lines drawn by the routine.

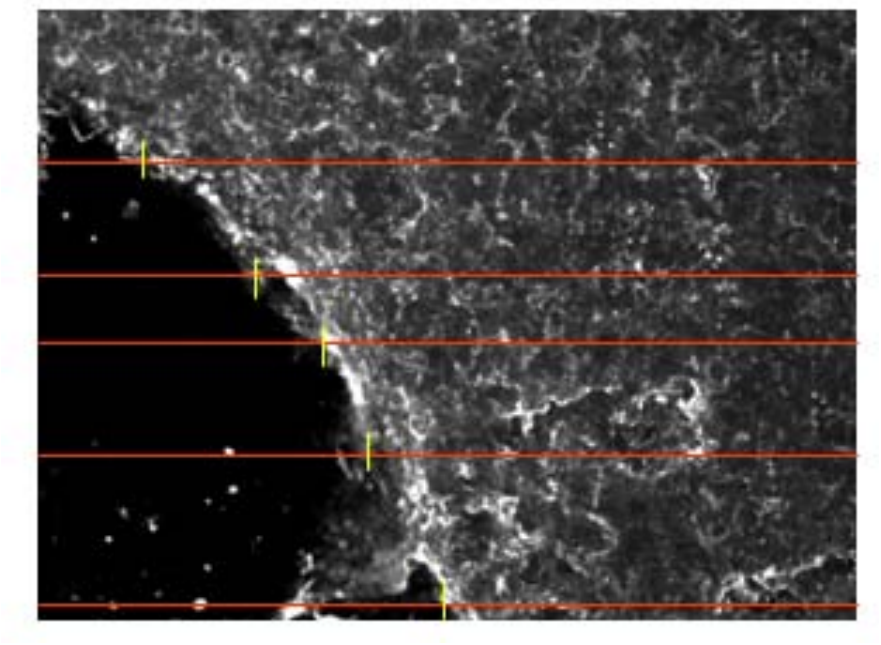

Figure 7: Visual Representation of Line Intensity Analysis

Example of an microelectrode hole quadrant analyzed in a unique MATLAB routine to determine GFAP expression (magnification 10x). Astrocytes can be specifically stained against GFAP and this staining is proportional to cell proliferation and level of hypertrophy. However, it is difficult to quantify this staining through traditional cell counting methodology. Therefore, we utilized a line intensity spectrum of magnitude of staining along a horizontal line across the image. Five randomly placed lines are drawn (shown in red) and the intensity displayed. These intensities are then zeroed with the edge of the hole chosen as the distance 0 (shown in yellow). The data compiled from these five lines can then be averaged and statically analyzed to determine differences between the porous images and the nonporous images.

In order to capture information of both cell proliferation and level of cell hypertrophy, the MATLAB routine processes a series of steps for each image. First, the image must be opened in the routine by a user. Next, it must be specified whether the

image was taken of the right or left side of the microelectrode hole because this will flip the alignment of the tissue and the blank space on the image.

Once the image is opened and the side is specified, the program places five horizontal lines randomly across the image (artificially shown in red in Figure 7) and the intensity of staining is quantified on an arbitrarily determined intensity scale that is consistent for all images analyzed in the system. This intensity profile generates an intensity value for each pixel along the line. Then, the user views a graphical representation of the line intensity to determine the edge of the hole and zero the data at this edge (artificially shown in yellow in Figure 7). See Figure 8 for an example of the intensity profile used.

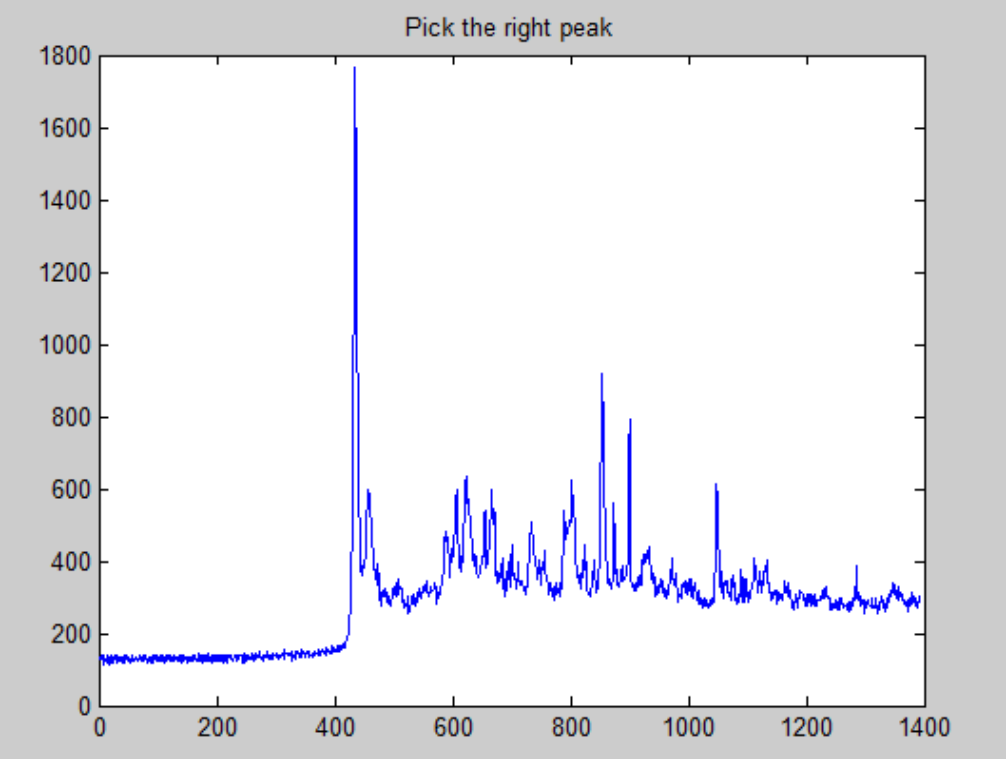

Figure 8: Graphical Representation of Intensity Profile

In this graphical representation of the intensity profile, the user must pick the edge of the hole, which is characterized by a very low intensity followed by large peak as the image transitions from the empty space of the microelectrode track to the bright staining of the compact astrocytic sheath surrounding the hole.

It is important to zero the data points to the edge of the hole for two reasons. The first is that the information desired is the cellular character at given distances from the edge of the microelectrode. The edge of the image is an arbitrary set point where as zeroing all data with the edge of the hole allows all line intensities to be combined and analyzed with regard to their distance from the microelectrode. The second reason for zeroing the data points in this way is that any intensity artifacts or loose tissue in the space of the hole is irrelevant to the data analysis and should be removed.

Once the data is obtained and zeroed, the data from these five lines can then be averaged and statistically analyzed to determine the effect of microelectrode treatment. Figure 9 shows both the histological image and graphical representation of the binned average intensity profile for a typical image. To determine if the difference in GFAP up-regulation around these surfaces was statistically significant, a paired t-test or an ANOVA was implemented. To assess the effect of porous silicon as a function of distance from the edge of the hole, a two-way ANOVA was performed. This analysis was done at one week. For the the two, four, and six week data, we were only interested in the difference between PS and smooth and we therefore performed a paired t-test. A paired, two tailed t-test was appropriate because each microelectrode contained both types of surface and the tissue was maintained in the original pairing for data analysis. It should be noted that this type of within subject control is important due to the inherently variable nature of in vivo data and the relatively modest sample size that can be obtained due to housing and cost constraints of maintain the animals.

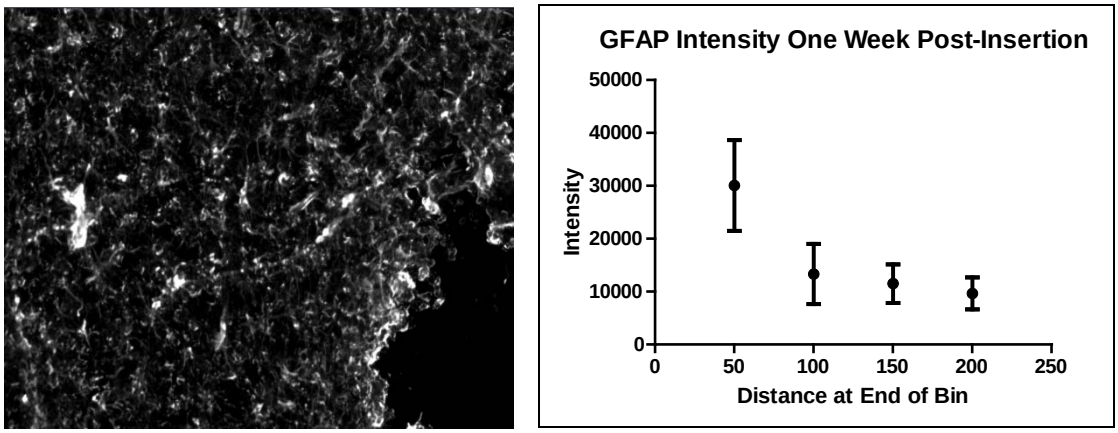

Figure 9: Example Output of Intensity Profile Protocol

The image on the left represents the histological image obtained of one quarter of a typical microelectrode track. The graph on the right shows GFAP specific staining intensity of this histological image.

7. RESULTS

Two animals were implanted with Spire Sample Type 7 mock microelectrode tips (100 µm diameter, 7 mm long). The samples were implanted into the cortex of the rats, which were sacrificed after one week. The brains were removed and stained for glia (GFAP), microglia/macrophages (ED-1), and healthy neurons (NeuN). An example of this staining can be seen in Figure 10.

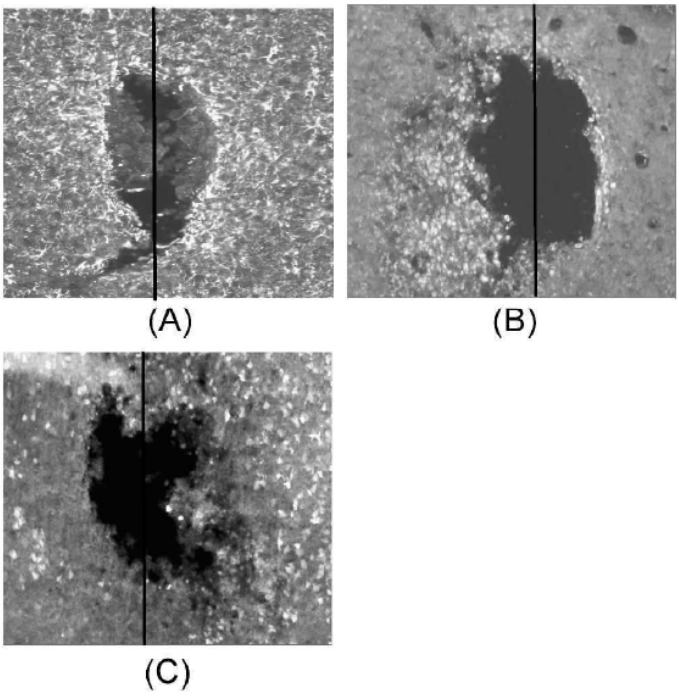

Figure 10: Immunohistochemical Staining Adjacent to Implanted Device at One Week Post-Insertion

Immunohistochemical staining adjacent to PS devices (‘mock’ microelectrodes), where one side (left on each panel) is smooth and the other (right) is nanostructured porous silicon (nPS). (A) GFAP expression, which marks astrocytes, showing less staining on the nPS side than the smooth side. (B) ED1, which stains for macrophages and microglia expression, is significantly reduced on the porous side of the microelectrode compared to the smooth side. (C) NeuN staining, which marks neurons, shows significantly more staining on the nPS side than the smooth side. This particular animal was killed one week after the PS device was implanted. The black line was added to show how the smooth side was discriminated from the porous silicon.

The staining intensity for GFAP for the tissue adjacent to the smooth surface was consistently higher than the staining adjacent to the porous silicon surface, but the difference did not reach statistical significance ($P = 0.054$, $F = 3.75$, $n = 217$) (Figure 11A). As expected, as the distance from the device increased, the intensity of the GFAP staining decreased and this difference was significant ($P < 0.001$, $F = 6.4$, $n = 217$). This

result is similar to other studies that showed an increase in glial activation near the microelectrode.

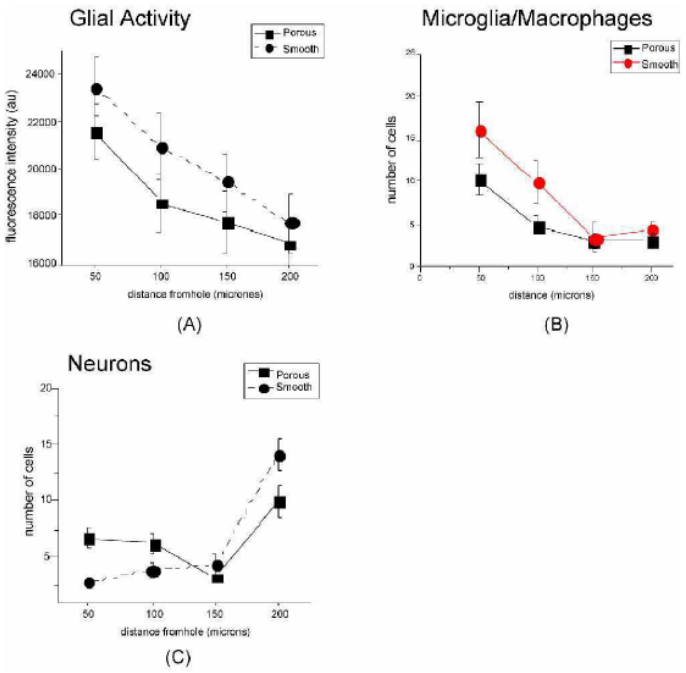

Figure 11: Graphical Representation of Tissue Reaction to Microelectrode Insertion at One Week Post-Insertion

Decreased glial activation and increased neurons adjacent to the porous silicon surface compared to smooth surfaces. (A) Astrocyte activation around each microelectrode hole was quantified by measuring the fluorescence intensity within 50 µm increments from the edge of the hole left by the microelectrode (refer to the methods and design component sections for details). While the florescence intensity adjacent to the porous silicon surface was consistently less than that around the smooth surface, the differences were not significantly different at any distance. (B) Microglia and macrophage activation around each microelectrode hole was significantly greater adjacent to the porous silicon surface than the smooth surface. (C) Neurons were more likely adjacent to the porous silicon surface than the smooth surface within 150 µm from the edge of the PS device. However, by 200 µm, there were fewer neurons adjacent to the porous silicon surface compared to the smooth surface.

In addition to quantifying the GFAP intensity around the devices, we also quantified the number of ED-1 positive cells around the device. Similar to the GFAP staining, the amount of ED-1 staining adjacent to the smooth surface was greater than the staining around the porous surface but this difference was significant ($P = 0.01$, $F = 6.66$, $n = 89$) (Figure 11B). In a manner similar to the GFAP staining, as the distance from the device is increased, the number of ED-1 positive cells also significantly decreased for the tissue around both the smooth and porous surfaces ($P < 0.001$, $F = 12.77$, $n = 89$). The significant difference in ED-1 staining around the porous surface compared to the ED-1 staining around the smooth surface suggest that modifying the surface of the microelectrode is sufficient to alter the up-regulation of microglia and recruitment of macrophages around a microelectrode.

Finally, we quantified the NeuN staining around the device and counted the number of positively-stained cells. Similarly for GFAP and ED-1 staining, there was a significant effect for distance from the PS device ($P < 0.001$, $F = 29.81$, $n = 237$) but the number of neurons increased as the distance from the PS device increased, the opposite from the decreases in GFAP or ED-1-positive staining, as one might expect (Figure 11C). There was also a significant interaction between distances from the PS device and the porous vs. smooth side of the device ($P < 0.001$, $F = 6.84$, $n = 237$). Post-hoc test revealed significantly more NeuN positive cells adjacent to the porous surface than adjacent to the smooth surface ($P < 0.001$) within 50 μm of the PS device. This difference decreased at 100 μm ($P = 0.050$) and was gone by 150 μm. At 200 μm, there were significantly fewer neurons adjacent to the porous silicon surface compared to the smooth surface. Therefore, modifying the surfaces of the microelectrodes not only reduces the

up-regulation of microglia and recruitment of macrophages but also increases the number of healthy neurons within recording distance around the recorded neurons (within 100 µm).

Taken together, these data suggest that the porous surfaces influence the glial scar formation and support the health of neurons at one week post insertion. Thus, the bioactive properties of nanostructured porous silicon identified by previous experiments by this lab in vitro can be maintained in vivo at one week post insertion.

To further analyze the effects of the porous surface found in vivo at one week post insertion, animals were implanted with Spire sample type 7 mock microelectrode tips (100 µm diameter, 7 mm long) and were sacrificed at 2, 4, or 6 weeks post insertion. The GFAP staining was analyzed to further study the consistent, but at one week not statistically significant, decrease in GFAP specific staining surrounding the microelectrode shaft. In this way, it was possible to determine if the lack of statistical significance in this decrease, at one week post insertion, was due to truly statistically insignificant circumstances or to data that was not robust enough.

Table 2: Summary of Experimental Units and Conditions
This table depicts a summary of experimental units at each of the time points. During tissue processing, some tissue samples were damaged and could not be analyzed.

Weeks	Number of Experimental Units (Animals)	Number of Tissue Slices Analyzed	Intensity Line Profiles Obtained
2	2	12	90
4	2	16	140
6	1	12	90

At two weeks post insertion, there was the most inconsistency in GFAP staining intensity. At 0-50 µm, 100-150 µm, and 150-200 µm, the GFAP staining intensity adjacent to the porous surface was greater on average but not significantly different from the smooth surface (Figure 12). However, at 150-200 µm, the intensity of the GFAP staining was significantly greater around the PS surface than the smooth surface ($p<0.05$). These findings are inconsistent with results at one week, four weeks, and six weeks and at this time, there is no evidence to explain these findings. More experimentation is required to determine if the cellular mechanisms acting in the two week post insertion timeframe are unique or if these results are anomalous.

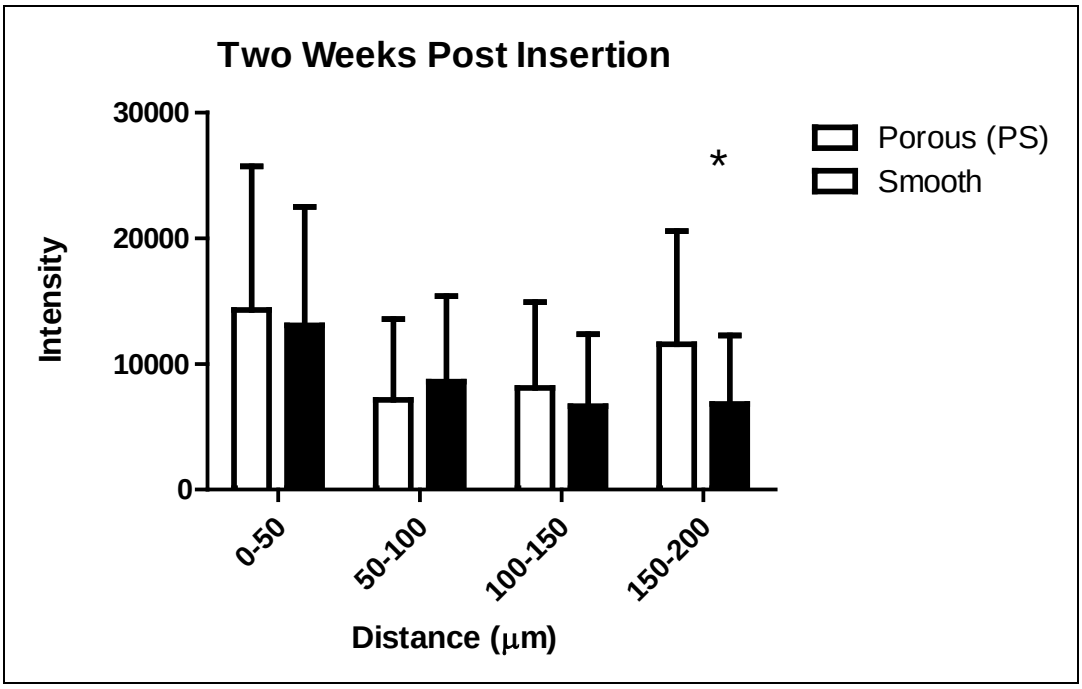

Figure 12: Graphical Representation of Tissue Reaction to Microelectrode Insertion at Two Weeks Post-Insertion

Graphical representation of GFAP staining intensity as distance from the microelectrode track increases at two weeks post insertion. The asterisk represents a significance difference in GFAP staining intensity ($p<0.05$).

At four weeks post insertion, there was roughly equivalent GFAP intensity at 0-50 μm and 50-100 μm adjacent to the porous surface and the smooth surface (Figure 13). However, as the distance from the microelectrode track increases to 100-150 μm, the average GFAP intensity is less adjacent to the porous surface as compared to the smooth surface and this difference approaches significance but is not significant by our cut off value ($p=0.086$). As the distance from the microelectrode track then increases to 150-200 μm, the average GFAP intensity is significantly less adjacent to the porous surface as compared to the smooth surface and this difference is significant ($p<0.05$). This would suggest that, at four weeks post insertion, the decrease in average GFAP intensity adjacent to the porous surface at one week post insertion is beginning to disappear but

that the decrease in average GFAP intensity at further distances (100-200 μm) becomes significant from the cellular processes occurring between one and four weeks. This may be due to the fact that the total recruitment of astrocytic cells is less in proximity to the porous surface but other factors are still contributing to the effects in very close proximity to the electrode.

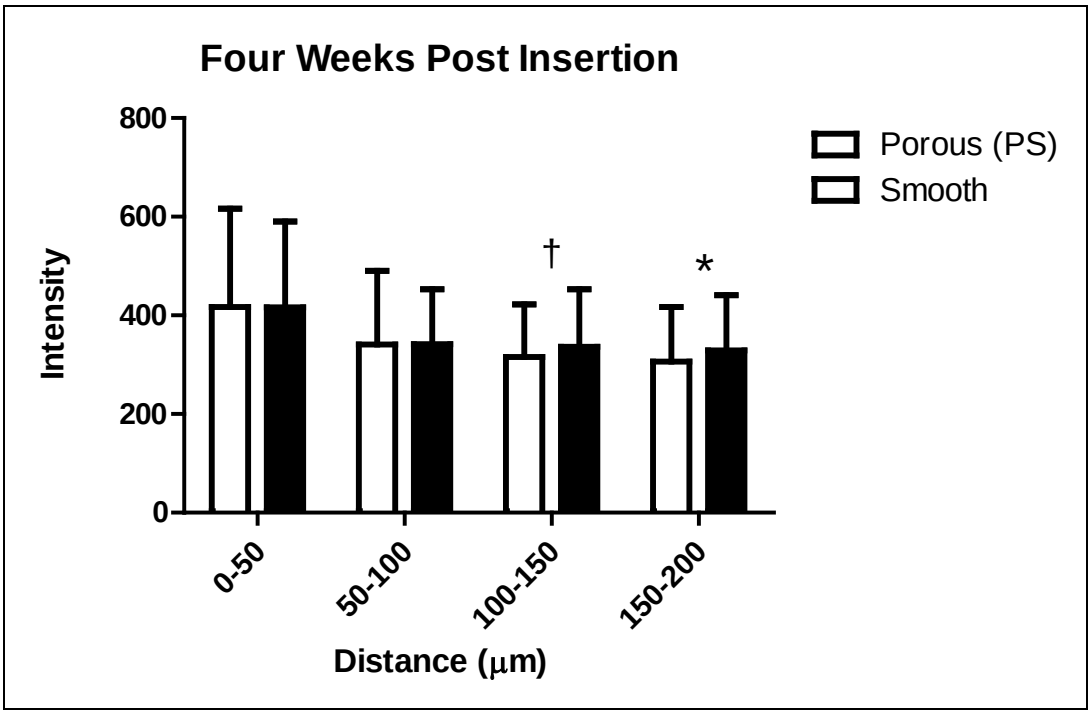

Figure 13: Graphical Representation of Tissue Reaction to Microelectrode Insertion at Four Weeks Post-Insertion

Graphical representation of GFAP staining intensity as distance from the microelectrode track increases at four weeks post insertion. The asterisk represents a significance difference in GFAP staining intensity ($p<0.05$). The cross represents a p value approaching statistical significance ($p=0.086$).

At six weeks post insertion, there is a decrease in GFAP staining intensity adjacent to the porous surface as compared to the smooth surface in all distance

increments from the microelectrode track (Figure 14). This difference is significant from 0-50 μm ($p<0.05$) and approaches significance at 50-100 μm ($p = 0.078$). However, this difference is not significant from 100-200 μm. Taken in context with the results from four weeks post insertion, these data suggest that all traumatic damage inflicted during microelectrode insertion has been mitigated and the chronic response to the microelectrode has begun. In this way, lower average intensity adjacent to the porous surface may be directly due to more favorable cellular response to the nanostructured surface. Moreover, the fact that this difference is only significant in close proximity to the microelectrode should be expected, as the further the distance is from the microelectrode track, the less interaction the cells have with the surface itself.

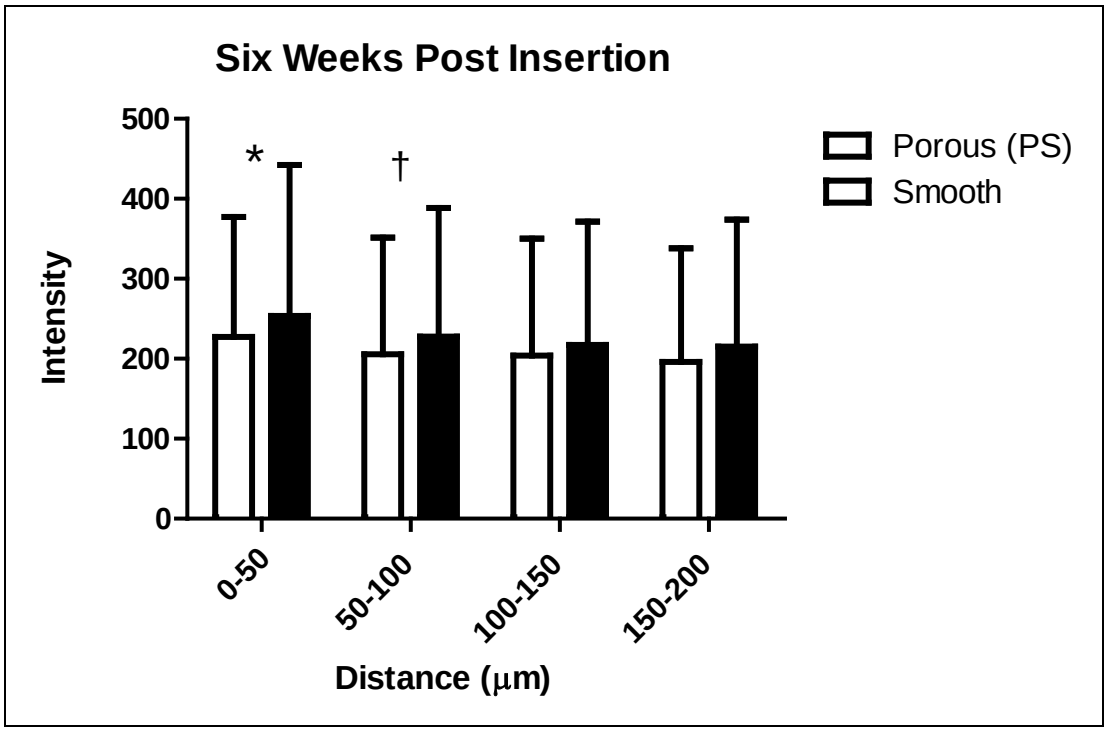

Figure 14: Graphical Representation of Tissue Reaction to Microelectrode Insertion at Six Weeks Post-Insertion

Graphical representation of GFAP staining intensity as distance from the microelectrode track increases at six weeks post insertion. The asterisk represents a significance difference in GFAP staining intensity ($p<0.05$). The cross represents a p value approaching statistical significance ($p=0.078$).

8. DISCUSSION

The prior work done by this lab, in vitro, to validate improved biocompatibility of porous microelectrode surfaces was validated in vivo by work completed for this thesis. Tissue around the microelectrode at one week post insertion had a lower density of glia and activated microglia/macrophages and more neurons. At six weeks post insertion, the tissue around the microelectrode has a lower density of glia closest to the microelectrode. These data—together with the in vitro data obtained in prior experiments—suggest that nanostructured materials will make a good surface for microelectrodes and should be tested for chronic periods on real microelectrodes so that their effect on actual neural recordings can be made. Correlations between histological analysis of cellular up-regulation and loss of discriminable single unit action potentials will provide an important bridge to understanding how cellular up-regulation affects neuronal recordings. Additionally, while there is less glial activation in the tissue adjacent to the porous silicon side at one, four, and six weeks, further work must be done using fabricated microelectrodes to test the ability to increase the number and duration of viable recording sites.

Utilizing our unique design for quantitatively assessing cell regulation around the microelectrode, we have shown successful quantification of astrocyte up-regulation in the brain tissue surrounding the site of microelectrode insertion. This is an important aspect of understanding the effects of cell morphology, not just cell count, imparted by the astrocytes surrounding the microelectrode. Therefore, future work done to improve the biocompatibility of inserted recording microelectrodes can be adequately assessed. This process of assessing the cellular response will aid in the creation of a more biocompatible

microelectrode and could help bring the therapeutic benefits of implanted recording microelectrodes to human patients.

Obtaining extracellular electrical potential recordings from microelectrodes implanted in mammalian cortex requires the electrical fluctuation due to changes in membrane potential of neurons to occur near the recording microelectrode. This allows for a recording of the sum of the electrical activity around the recording site to be obtained. Therefore, if the microelectrode is close enough to a cell of interest, usually within 100 μm, the potential change due to an action potential can be recorded. However, if the microelectrode is too far away, the amplitude of the action potential degrades and is corrupted by other potential changes from other cells and can no longer be discriminated from the background activity. Therefore, the recording site of the microelectrode must remain very close to the neurons. Since the statistical significance of a decrease in astrocytic up-regulation increases in the range of 0-100 μm as the time post-insertion approaches the chronic state (six weeks), this would suggest that the porous surface induces more favorable reaction for chronic insertion. Unfortunately, although the decrease is statistically significant, more work will be needed to determine if this difference is biologically significant. The difference in up-regulation imparted by the porous surface is likely not to be great enough in magnitude to maintain a fully uninterrupted microelectrode-tissue interface. Additionally, insertion of the microelectrode devices not only induces gliosis, but this process reduces the density of neurons around the microelectrode and this will likely require multiple approaches to alleviate.

The significant decrease in all types of glial staining as the distance from the PS device increases at one week post insertion suggests that there is a significant up-regulation of these cell types in response to the microelectrode insertion. While one might initially expect that no increase in glial activation is the most desirable state after microelectrode insertion but this is unlikely to be this case. The initial insertion of the microelectrode will damage neurons, tear dendritic and axonal processes, and perhaps cause some cell death. Damage to the blood brain barrier (BBB) is also likely. The fact that the up-regulation of glial cell types was less adjacent to the porous silicon surfaces compared to the smooth surface suggests the porous surface is more supportive of damaged neurons, and less likely to further induce glial up-regulation due to foreign body responses. This was supported by data at longer time points, with special emphasis on six weeks post insertion, where decrease in glial up-regulation was significant close to the microelectrode track. However, more experimentation is needed to determine if the data obtained at two weeks post insertion was anomalous with regards to glial up-regulation or if other factors during this time period affect the response.

Negative correction between glial cell types and neurons at one week post insertion suggests that perhaps the increase in glia pushes the neurons away from the microelectrode. The fact that, at 200 μm, there were significantly more neurons on the side adjacent to the smooth microelectrode supports this idea that neurons are pushed away rather than dying. If neurons are pushed away, the fewer that exist near the recording site, the more there must be at some distance further from the recording site surface. Although more work is needed to confirm this, it is likely that the nanostructured porous surfaces are less likely to push the neurons away than a smooth surface.

It is important to note that it is unlikely that modifying the surface alone will be sufficient to maintain single neuron recordings for neurorobotic applications in humans. There are two major effects of chronically implanting arrays of microelectrodes into the brain. The first is due to the action of inserting the microelectrode through the tissue that will damage and tear neuronal and glial processes, exposing the extracellular environment to intracellular proteins and damaging the BBB. The exposure of the extracellular environment to both intracellular and blood proteins initiates a cascade of events that can help to remove the damaged tissue and debris and heal the tissue or, if the damage is severe, create a glial scar that walls of the microelectrode from recording single neurons.

The second major effect is the continued existence of the microelectrode in the neural tissue, commonly referred to as the foreign body response. If the brain is subject to a stab wound with a device about the size of a microelectrode (meaning that the device is inserted into the tissue, withdrawn and the dura and skull replaced), the wound will heal within six months. Therefore, it will be difficult to identify the location of the wound if the stab was done under controlled, sterile conditions. However, if the device used to create the stab wound is left in place, a glial scar will form around the device, effectively walling it off from the healthy neural tissue.

The discussion of future experimentation addresses possible avenues for maintaining single neuron recordings for longer periods of time via application of coating to the surface of the microelectrode. These coatings work to decrease the adverse consequences of both effects of microelectrode insertion.

9. LIMITATIONS

Intensity Analysis

The utilization of line intensity analysis addresses many of the shortcomings of other methods in quantifying astrocytic up-regulation. However, there are shortcomings of this method that should be addressed as well. These shortcomings involved the variations of intensity between different days of staining and image capture. Therefore, with different background intensity on different days, cross comparison of the different groups of images may be hindered. In an attempt to minimize the effects of this, strict controls were maintained during tissue treatment, processing, and image capture to assure smallest possible deviations in background intensity.

Also, as the electrode track is roughly circular, the use of horizontal lines do not actually yield the true radial distance from the edge of the track. There would be no feasible way to implement the use of radial intensity lines in an automated fashion with our software and therefore it may be prohibitively difficult to fix. However, the division of the image into four quadrants minimizes some of the curvature of the electrode hole (as compared to having the entire hole in one image) and this should mitigate the small difference between the horizontal and radial distance.

Use of Mock Microelectrode Tips

Due to the prohibitively high cost of the manufacturing of microelectrodes, experimentation was completed with relatively thick porous silicon wafers (100 µm) diced into shafts, 100 µm wide, to produce a device of 100 µm square. While we expect our final device to be less than 50 µm in diameter, previous work has suggested that 1devices up to 500 µm do not increase the thickness of the glial scar, we felt confident in initial testing of these larger devices in vivo.

10. FUTURE WORK

Better Understanding of Chronic Time Points

Due to the anomalous data obtained at two weeks post insertion, further experimentation should analyze the cellular reaction to microelectrode insertion during this time frame. Additionally, further experimentation should be completed to analyze the activity of neurons and macrophages at the longer time points of two, four, and six weeks. If success is seen at these time points, electrically viable microelectrodes should be implanted for longer periods of time on the order of months. These experiments will be able to combine the methods utilized in this paper to quantify the cellular response with loss of ability to record single unit action potentials in vivo.

Novel Surface Treatments

Future studies should also be completed to determine appropriate surface treatments to augment microelectrode biocompatibility. Many groups have completed experimentation showing improved biocompatibility from novel surface treatments. Additionally, the porous surface of our microelectrode may allow for a higher volume of surface treatment to be coating onto the microelectrode as these coating may move into the porous when applied via natural capillary action or other techniques.

Future studies, stimulated by previous work from this lab, could analyze the efficacy of novel surface coatings to improve the biocompatibility of porous

microelectrodes in the brain. Poloxamer is one proposed novel surface treatment that has been utilized in the related field of traumatic brain injury to mitigate the effects of trauma. Currently, a study is underway to determine the effects of coating the microelectrode with Poloxamer 188 prior to insertion. At two, four, and six weeks post insertion, histology will be completed to determine the effects of this surface treatment on porous surfaces to increase neuronal survival and decrease glial up-regulation and macrophage/microglia recruitment.

In one pilot study completed, we used laminin to coat the tips of the microelectrodes in order to make the relatively smooth and biologically foreign silicon more adapted to the brain environment. A laminin coating was used on half of the microelectrodes implanted, compared to saline control. Laminin was chosen because, although it is not present in the healthy brain tissue, it is an important aspect of the extracellular matrix in other body tissues and has been shown to be useful in cellular culture of neurons. To apply the laminin coating to the microelectrode, the microelectrode tips were soaked in a 10% laminin dilution in PBS overnight under an ultraviolet sterile hood. Application of this technique to a porous microelectrode treated may have the potential to further improve biocompatibility.

Additionally, Brain Derived Neurotropic Factor (BDNF) has been studied in pilot work in this lab to improve the biocompatibility of porous microelectrodes in the brain. BDNF is a naturally occurring brain hormone involved in differentiation of brain cell types and healthy cellular growth in the healthy brain. BDNF is also utilized in cell culture to force differentiation of neural progenitors into a variety of neuronal cell types. To apply the BDNF coating to the microelectrode, microelectrode tips were soaked in

1:100 dilution of BDNF in PBS for two hours prior to insertion under an ultraviolet sterile hood. Application of this technique to a porous microelectrode may have the potential to further improve biocompatibility.

11. CONCLUSION

Knowledge of both the effects of microelectrode insertion and the foreign body response does not immediately lead us to a solution for implantation of the microelectrodes. While some of the factors that contribute to this scar (size of the device inserted, speed of insertion, etc.) and mechanisms of scar formation (recruitment of macrophages, activation of microglia, etc.) have been well studied, the relationship between single neuron recording and glial scar formation are less well understood. We hypothesize that these two effects (electrode insertion and foreign body response) interact such that despite the fact the loss of recordings occurs months after implantation, processes initiated during the early phase of the response persist and contribute to the eventual encapsulation of the microelectrode. This idea is supported by studies on traumatic brain injury, demonstrating that mechanical trauma can initiate progressive degeneration, which continues long after the traumatic event. We expect that using a bioactive surface (nanostructured porous silicon), possibly in conjunction with novel surface coatings that help ameliorate damage to neurons due to the microelectrode insertion, will ultimately allow for a device that can maintain close contact of neurons to the recording sites and allow for very long term neuronal recordings.

12. LIST OF REFERENCES

Anderson, JM, Rodriquez A, and Chang DT. "Foreign body reaction to biomaterials." *Seminars in immunology* 20.2 (2008):86-100.

Araque, A, Sanzgiri RP, Parpura V, and Haydon PG. "Astrocyte-induced modulation of synaptic transmission." *Canadian journal of physiology and pharmacology* 77(1999):699-706.

Azemi, E, Stauffer WR, Gostock MS, Lagenaur CF, and Cui XT. "Surface immobilization of neural adhesion molecule L1 for improving the biocompatibility of chronic neural probes: In vitro characterization." *Acta biomaterialia* 4.5 (2008):1208-1217.

Babcock, AA, Kuziel WA, Rivest S, and Owens T. "Chemokine expression by glial cells directs leukocytes to sites of axonal injury in the CNS." *The journal of neuroscience* 23.21 (2003):7922-7930.

Biran, R, Martin DC, and Tresco PA. "Neuronal cell loss accompanies the brain tissue response to chronically implanted silicon microelectrode arrays." *Experimental neurology* 195.1 (2005):115-26.

Buchko CJ, Kozloff KM, Martin DC. “Surface characterization of porous, biocompatible protein polymer thing films.” *Biomaterials* 6.11 (2001): 1289-300.

Cheung KC, Djupsund K, Dan Y, Lee LP. “Implantable Multichannel Electrode Array Based on SOI Technology.” *Journal of microelectromechnical systems* 12:2 (2001):179-184.

Cui X, Lee VA, Raphael Y, Wiler JA, Hetke JF, Anderson DJ, Martin DC. "Surface modification of neural recording electrodes with conducting polymer/biomolecule blends." *Journal of biomedical materials research* 56.2 (2001):261-272.

Cui Q, Pollett MA, Symons NA, Plant GW, Harvey AR. "A new approach to CNS repair using chimeric peripheral nerve grafts." *Journal of neurotrauma* 20.1 (2003):17-31.

Doroski DM, Brink KS, and Temenoff JS. "Techniques for biological characterization of tissue-engineered tendon and ligament." *Biomaterials* 28.2 (2007):187-202.

Edell DJ, Toi VV, McNeil VM, Clark LD. “Factors Influencing the Biocompatibility of Insertable Silicon Microshafts in Cerebral Cortex.” *IEEE Transactions on Biomedical Engineering* 39.6 (1992):635-643.

Elkabes S, DiCicco-Bloom EM, and Black IB. "Brain microglia/macrophages express neurotrophins that selectively regulate microglial proliferation and function." *The journal of neuroscience* 16.8 (1996):2508-2521.

Fawcett JW and Asher RA. "The glial scar and central nervous system repair." *Brain research bulletin* 49.6 (1999):377-391.

Fitch MT and Silver J. "Activated macrophages and the blood-brain barrier: inflammation after CNS injury leads to increases in putative inhibitory molecules." *Exp neurol.* 148.2 (1997):587-603.

Fitch MT, Doller C, Combs CK, Landreth GE, Silver J. "Cellular and molecular mechanisms of glial scarring and progressive cavitation: in vivo and in vitro analysis of inflammation-induced secondary injury after CNS trauma." *Journal of neuroscience* 1;19.19 (1999):8182-8198.

Goss JR, O ME. "Astrocytes are the major source of nerve growth factor upregulation following traumatic brain injury in the rat." *Experimental neurology* 149.2 (1998):301-9.

Giulian D, Baker TJ, Shih LN, Lachman LB. "Interleukin 1 of the central nervous system is produced by ameboid microglia." *The Journal of experimental medicine* 164.2 (1986):594-604.

Giulian D, Li J, Leara B, Keenen C. "Phagocytic microglia release cytokines and cytotoxins that regulate the survival of astrocytes and neurons in culture." *Neurochem int.* 25.3 (1994):227-233.

He W, McConnell GC, and Bellamkonda RV. "Nanoscale laminin coating modulates cortical scarring response around implanted silicon microelectrode arrays." *Journal of neural engineering* 3.4 (2006):316-326.

Hochberg LR, Serruya MD, Friehs GM, Mukand JA, Saleh M, Caplan AH, Branner A, Chen D, Penn RD, Donoghue JP. "Neuronal ensemble control of prosthetic devices by a human with tetraplegia." *Nature* 442(2006):164-171.

Horbett T. "The role of adsorbed proteins in tissue response to biomaterials." In: Ratner B, et al., editors. Biomaterials science: an introduction to biomaterials in medicine. San Diego, CA: Elsevier Academic Press; (2004):237–246.

Hynd MR, Frampton JP, Dowell-Mesfin N, Turner JN, Shain W. "Directed cell growth on protein-functionalized hydrogel surfaces." *Journal of neuroscience methods* 162.1-2 (2007):255-263.

Jun SB, Hynd MR, Dowell-Mesfin NM, Al-Kofahi Y, Roysam B, Shain W, Kim SJ. "Modulation of cultured neural networks using neurotrophin release from

hydrogel-coated microelectrode arrays." *Journal of neural engineering* 5.2 (2008):203-213.

Kerns BJ, Jordan PA, Moore MH, Humphrey PA, Berchuck A, Kohler MF, Bast RC, Iglehart JD, Marks JR. "p53 overexpression in formalin-fixed, paraffin-embedded tissue detected by immunohistochemistry." *The journal of histochemistry and cytochemistry* 40.7 (1992):1047-1051.

Kim DH and Martin CD. "Sustained release of dexamethasone from hydrophilic matrices using PLGA nanoparticles for neural drug delivery." *Biomaterials* 27.15 (2006):3031-3017.

Kim KH and Kim SJ. “Method for unsupervised classification of multiunit neural signal recording under low signal-to-noise ratio.” IEEE trans biomed eng. 50.4 (2003):421-431.

Klaver CL and Caplan MR. "Bioactive surface for neural electrodes: Decreasing astrocyte proliferation via transforming growth factor-β1." *Journal of biomedical materials research* Part A 81a.4 (2007):1011-1016.

Kossman T, Hans V H, Imhof H G, Stocker R, Grob P, Trentz O, Morganti-Kossman C. “Intrathecal and serum interleukin-6 and the acute-phase response in patients with severe traumatic brain injuires.” Shock 4.5 (1995):311-317.

Landis DMD. “The early reactions of nonneuronal cells to brain injury.” *Annu rev neurosci* 17. (1994):133–151.

Leung BK, Biran R, Underwood CJ, Tresco PA. "Characterization of microglial attachment and cytokine release on biomaterials of differing surface chemistry." *Biomaterials* 29.23 (2008):3289-97.

Ling E. “The origin nature of microglia.” In: Federoff S, editor. *Advances in cellular neurobiology*. Orlando: Academic Press; 1981. p. 33–82.

Liu X, McCreery DB, Carter RR, Bullara LA, Yeun TGH, Agnew WF. “Stability of the interface between neural tissue and chronically implanted intracortical microelectrodes.” *IEEE trans. rehabil. eng.* 7 (1999): 315.

Ludwig KA, Uram JD, Yang J, Martin DC, and Kipke DR. "Chronic neural recordings using silicon microelectrode arrays electrochemically deposited with a poly (3, 4-ethylenedioxythiophene)(PEDOT)." *Journal of neural engineering* 3.1 (2006):59-70.

McKenzie JL, Waid MC, Shi R, Webster TJ. “Decreased functions of astrocytes on carbon nanofiber materials.” *Biomaterials.* 25 (2004), 1309-1317.

McNally AK and Anderson JM. “Beta1 and beta2 integrins mediate adhesion during macrophage fusion and multinucleated foreign body giant cell formation.” *Am J pathol* 160.2 (2002):621–30.

Merrill DR and Tresco PA. 2005 “Impedance Characterization of Microarray Recording Electrodes in Vitro.” *IEEE Transactions on Biomedical Engineering* 52.11 (2005): 1960-1965.

Minghetti L and Levi G. “Microglia as effector cells in brain damage and repair: focus on prostanoids and nitric oxide” *Prog neurobiol* 54.1 (1998): 99-125.

Moore K, Macsween M, and Shoichet M. "Immobilized concentration gradients of neurotrophic factors guide neurite outgrowth of primary neurons in macroporous scaffolds." *Tissue engineering* 12.2 (2006):267-278.

Moxon KA. “Multichannel electrode design: Considerations for different applications in Methods for simultaneous neuronal ensemble recordings.” 25-45 Eds. M.A.L. Nicolelis CRC Press Boca Raton FL 1999.

Moxon KA, Hallman S, Aslani A, Kalkhoran NM, Lelkes PI. "Bioactive properties of nanostructured porous silicon for enhancing electrode to neuron interfaces." *Journal of biomaterials science Polymer edition* 18.10 (2007):1263-81.

Moxon KA, Leiser S C, Gerhardt G A, Barbee K, Chapin J K. “Ceramic based multisite electrode arrays for electrode recording.” *IEEE Trans. Biomed. Eng.* (2004).

Moxon KA, Kalkhoran NA, Markert M, Sambito MA, McKenzie JL, Webster JT. “Nanostructured surface modification of ceramic-based microelectrodes to enhance biocompatibility for a direct brain-machine interface.” *IEEE transactions on bio-medical engineering* 51.881 (2004).

Nakajima K, Honda S, Tohyama Y, Imai Y, Kohsaka S, Kurihara T. "Neurotrophin secretion from cultured microglia." *Journal of neuroscience research* 65.4 (2001):322-331.

Nathaniel EJH and Nathaniel DR. The reactive astrocyte. In: Federoff S, editor. Advances in cellular neurobiology. Orlando: Academic Press; 1981. p. 249–301.

Nicolelis MAL, Dimitrov D, Carmena JM, Crist R, Lehew G, Kralik JD, Wise SP. "Chronic, multisite, multielectrode recordings in macaque monkeys." *Proceedings of the national academy of cciences of the united states of america* 100.19 (2003):11041-11046.

Polikov VS, Tresco PA, and Reichert WM. "Response of brain tissue to chronically implanted neural electrodes." *Journal of neuroscience methods* 148.1 (2005):1-18.

Porada I, Bondar I, Spatz WB, Kruger J. “Rabbit and monkey visual cortex: more than a year of recording with up to 64 microelectrodes.” *Journal of Neuroscience methods.* 95 (2000): 13-28.

Purves D, Augustine GJ, Fitzpatrick D, Katz LC, LaMantia A, McNamara J. Neuroscience. second ed. Sunderland: Sinauer Associates; 2001.

Raghupathi R, Graham DI, and McIntosh TK. “Apoptosis after traumatic brain injury.” *Journal of neurotrauma* 17.10 (2000):927-938.

Raivich G, Haas S, Werner A, Klein MA, Kloss C, Kreutzberg GW. “Regulation of MCSF receptors on microglia in the normal and injured mouse central nervous system: a quantitative immunofluorescence study using confocal laser microscopy.” *Journal of comparative neurology* 395.3 (1998):342-58.

Retterer ST, Smith KL, Bjornsson CS, Neeves KB, Spence AJH, Turner JT, Shane W, Isaacson MS. “Model Neural Prostheses With Integrated Microfluidics: A Potential Intervention Strategy for Controlling Reactive Cell and Tissue Responses.” *IEEE Transactions on Biomedical Engineering.* 51.11 (2004):2063-2073.

Retterer ST, Smith KL, Bjornsson CS, Turner JN, Isaacson MS, Shain W. "Constant pressure fluid infusion into rat neocortex from implantable microfluidic devices." *Journal of neural engineering* 5.4 (2008):385-391.

Richardson-Burns SM, Hendricks JL, Foster B, Povlich LK, Kim D, Martin DC. "Polymerization of the conducting polymer poly (3, 4-ethylenedioxythiophene) (PEDOT) around living neural cells." *Biomaterials* 28.8 (2007):1539-1552.

Schultz RL and Willey TJ. "The ultrastructure of the sheath around chronically implanted electrodes in brain." *Journal of neurocytology* 5.6 (1976):621-642.

Schwartz AB, Cui XT, Weber DJ, Moran DW. "Brain-controlled interfaces: movement restoration with neural prosthetics." *Neuron* 52.1 (2006):205-220.

Serbest G, Horwitz J, and Barbee K. "The effect of poloxamer-188 on neuronal cell recovery from mechanical injury." *Journal of neurotrauma* 22.1 (2005):119-132.

Serbest G, Horwitz J, Jost M, and Barbee KA. "Mechanisms of cell death and neuroprotection by poloxamer 188 after mechanical trauma." *The FASEB journal* (2005) 10.1096.

Seymour JP and Kipke DR. "Neural probe design for reduced tissue encapsulation in CNS." *Biomaterials* 28.25 (2007):3594-3607.

Shain W, Spataro L, Dilgen J, Haverstick K, Retterer S, Isaacson M, Saltzman M, Turner JN. "Controlling cellular reactive responses around neural prosthetic devices using peripheral and local intervention strategies." *IEEE transactions on neural systems and rehabilitation engineering* 11.2 (2003):186-188.

Sheng WS, Hu S, Kravitz F H, Peterson P K, Chao CC. "Tumor necrosis factor alpha upregulates human microglial cell production of interleukin-10 in vitro." *Clin diagn lab immunol.* 2.5 (1995):604-608.

Spataro L, Dilgen J, Retterer S, Spence AJ, Isaacson M, Turner JN, Shain W. "Dexamethasone treatment reduces astroglia responses to inserted neuroprosthetic devices in rat neocortex." *Experimental Neurology* 194.2 (2004):289-300.

Suner S, Fellows MR, Vargas-Irwin C, Nakata GK, Donoghue JP. "Reliability of signals from a chronically implanted, silicon-based electrode array in non-human primate primary motor cortex." *IEEE transactions on neural systems and rehabilitation engineering* 13.4 (2005):524-41.

Stauffer WR and Cui XT. "Polypyrrole doped with 2 peptide sequences from laminin." *Biomaterials* 27.11 (2006):2405-2413.

Stensaas SS and Stensaas LJ. "Histopathological evaluation of materials implanted in the cerebral cortex." *Acta neuropathologica* 41.2 (1978):145-155.

Streit WJ. Microglial cells. In: Kettenmann H, Ransom BR, editors. Neuroglia. New York: Oxford University Press; 1995. p. 85–95.

Szarowski DH, Andersen MD, Retterer S, Spence AJ, Isaacson M, Craighead HG, Turner JN, Shain W. "Brain responses to micro-machined silicon devices." *Brain research* 983.1-2 (2003):23-35.

Tomobe YI, Hama H, Sakurai T, Fujimori A, Abe Y, Goto K. "Anticoagulant factor protein S inhibits the proliferation of rat astrocytes after injury." *Neurosci Lett.* 16.214(1) (1996):57-60.

Turner GD, Ly V C, Nguyen T H, Tran T H, Nguyen H P, Bethell D, Wyllie S, Louwrier K, Fox S B, Gatter K C, Day N P, Tran T H, White N J, Berendt A R. "Systemic endothelial activation occurs in both mild and severe malaria. Correlating dermal microvascular endothelial cell phenotype and soluble cell adhesion molecules with disease severity." *Am J Pathol.* 152.6 (1998):1477-1487.

Turner JN, Shain W, Szarowski DH, Anderson M, Martins S, Isaacson M, Craighead H. "Cerebral astrocyte response to micromachined silicon implants." *Experimental neurology* 156.1 (1999):33-49.

Wiesmann C and de Vos AM. “Nerve growth factor: structure and function.” *Cell Mol Life Sci.* 58.5-6 (2001):748-759.

Winter JO, Cogan SF, and Rizzo JF. "Neurotrophin-eluting hydrogel coatings for neural stimulating electrodes." *Journal of biomedical materials research* 81b.2 (2007):551-563.

Woodroofe MN, Sarna G S, Wadhwa M, Hayes G M, Loughlin A J, Tinker A, Cuzner M L. “Detection of interleukin-1 and interleukin-6 in adult rat brain, following mechanical injury, by in vivo microdialysis: evidence of a role for microglia in cytokine production.” *Journal of neuroimmunology* 33.3 (1991):227-236.

Xiao Y, Martin DC, Cui X, Shenai M. “Surface modification of neural probes with conducting polymer poly (hydroxymethylated-3,4- ethylenedioxythiophene) and its biocompatibility.” *Appl biochem biotechnol* 128.2 (2006):117-130.

Zhong Y and Bellamkonda RV. "Controlled release of anti-inflammatory agent α-MSH from neural implants." *Journal of controlled release* 106.3 (2005):309-318.

Zhong Y and Bellamkonda RV. "Dexamethasone-coated neural probes elicit attenuated inflammatory response and neuronal loss compared to uncoated neural probes." *Brain research* 1148 (2007):15-27.